Ioannina, 31/01/2015

Dear Editor,

Enclosed please find the revised version of **acp-2014-374** paper entitled **"The regime of aerosol asymmetry parameter over Europe, Mediterranean and Middle East based on MODIS satellite data: evaluation against surface AERONET measurements"**. The manuscript has been revised taking carefully into account the comments of Reviewers 1 and 2 as well those of Dr A. M. Sayer. Based on their comments, specific emphasis was given to the discussion of uncertainties of MODIS aerosol asymmetry parameter and its long-term changes (new section 3.2.3 and two extra Figures – 7 and 8 – in the revised manuscript).

I also send you point-by-point responses to the comments of both Reviewers and A. M. Sayer.

Yours sincerely,

Nikos Hatzianastassiou

Dr Nikos Hatzianastassiou
Laboratory of Meteorology
Physics Department
University of Ioannina
45110 Ioannina
Greece

Tel: ++30 26510 08539
Fax: ++30 26510 08699
email: nhatzian@cc.uoi.gr

Response to A. M. Sayer

We would like to thank A. M. Sayer for his helpful comments regarding trends and Terra/Aqua differences. We carefully read through them and also the reported papers (Levy et al., 2010; 2013, Lyapustin, AMT, 2014) in his comment and took all of them into account in the revised version of our paper.

- Since the analysis was done with Collection 5 data, I expect that the trend in Terra data will be influenced (possibly quite strongly) by the calibration drift in that sensor. The differences between Terra and Aqua may likewise be a result of calibration differences. (combination of different absolute calibrations, and different drifts in various spectral channels in the two sensors). It is known that Collection 5 has an offset between Terra and Aqua in AOD, which changes through the mission. The asymmetry parameter information essentially depends on which aerosol modes are picked by the solution, and the relative weights between the two (i.e. it is more a derived quantity than the retrieved quantity). As this is largely a function of the spectral shape of reflectance, it is likely to be even more sensitive than AOD to calibration uncertainties.

Indeed, we were aware in our original document that there are calibration issues with the spectral channels of MODIS and that there is an optical sensor degradation, with the Terra suffering more than Aqua with regards to this. We acknowledge that these calibration drift issues and changes between Terra and Aqua are known to produce offsets between the two sensors and that, thus, may also generate similar differences in Terra and Aqua aerosol asymmetry parameter. Consequently, basically we tried to refrain from analysing the physical causes for the differences between the Terra and Aqua slopes of asymmetry parameter (Fig. 5, sect. 3.2.2) and to only refer to different time overpass time of the two platforms. However, we acknowledge that some statements made in the original manuscript may have been misleading with regards to this. Therefore, in order to avoid confusion, we have removed these statements in the revised version of the paper. Also, based on this A. M. Sayer comment, we made specific and extended reference to the MODIS calibration issues and its possible impacts on aerosol asymmetry parameter trends. In this sense, the results of Terra and Aqua aerosol asymmetry parameter trends presented in this paper (Fig. 5) are not to be taken as truth but rather they are given as a diagnostic of a problematic situation with MODIS aerosol asymmetry parameter. In line with this, inter-annual changes of asymmetry parameter are neither attempted nor derived based on the time-series of asymmetry parameter for the seven sub-regions of Fig. 6. All these are now stated in sect. 3.2.2, lines 366-377.

- I expect the new Collection 6 data will have resolved some of these issues, thanks to the work of the MODIS Calibration Science Team and Ocean Biology Processing Group in improving and maintaining the quality of MODIS calibration (both absolute and correction of drifts). Because of this, I would not try to interpret the Collection 5 Terra (and possibly Aqua, given the possibility of drift in later years) for trends, or to assign an Earth-related basis for differences between Terra and Aqua. My feeling is that calibration effects cannot be discounted here; repetition of the analysis with Collection 6 may be better (although I can't say for sure if calibration effects can be discounted entirely in C6).
Levy et al., AMT (2013). See Figure 15 for Ångström exponent changes between MODIS C5 and C6 (which, as it is also size-related information, may indicate changes in asymmetry parameter, although I don't know if anyone has looked at this in C6 yet). Note this is for Aqua data.

Accordingly to this comment, we have made a relevant statement (sect. 3.2.2, lines 377-382) referring to a possible, at least partly, solution of these calibration problem in the new Collection 006 MODIS product.

We would like to clarify that on the occasion of this important comment of A. M. Sayer, we tried to make a quick assessment of how aerosol asymmetry parameter inter-annual trends change in the new C006 data product (from C005). As of now, only the Aqua database is available while the corresponding one of Terra is in preparation. Nevertheless, no aerosol asymmetry parameter product was found in C006 data, which prevented us from making such a direct assessment. Therefore, we tried to use another aerosol size parameter and therefore we computed the Angstrom exponent (AE), which is the most common, using spectral aerosol optical depth data. The results given below are obtained from the performed analysis using the MODIS C005 and C006 AE at 550-865 nm wavelength pair, with data spanning the period 2002-2010.

First, emphasis is given on how the C005 and C006 AE data themselves (not their trends) compare to each other. From Fig. 1 and Fig. 2 a similarity is apparent in the main geographical patterns, which are also in line with those of asymmetry parameter in our paper (Fig. 2). For example, note the high AE values in the Black Sea (yellowish-reddish colors), indicative of fine aerosols, the relatively high values in the Mediterranean Sea (greenish-yellowish colors) and the low values (deep bluish colors) off the western African coasts corresponding to exported Saharan dust. The similarity between C005 and C006 AE data is also depicted in the computed correlation coefficients (Fig. 3), exceeding 0.8, and biases (in absolute and relative percentage terms, Figs 4 and 5, respectively) which are smaller than 0.1 or 10% in most areas of the study region and 0.2 or 20% almost everywhere. It should be noticed that our AE results are in line with those of Levy et al. (2013, Fig. 15) which refer, however, only to year 2008 (ours are for 2002-2010).

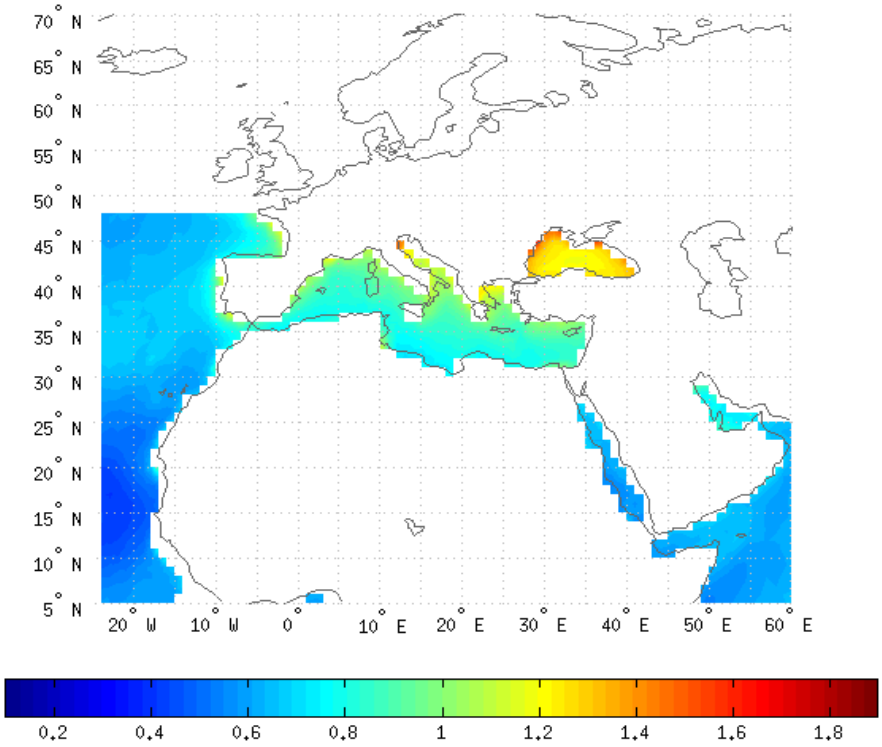

Figure 1. MODIS C005 Angström exponent at 550-865 nm for the period 2002-2010.

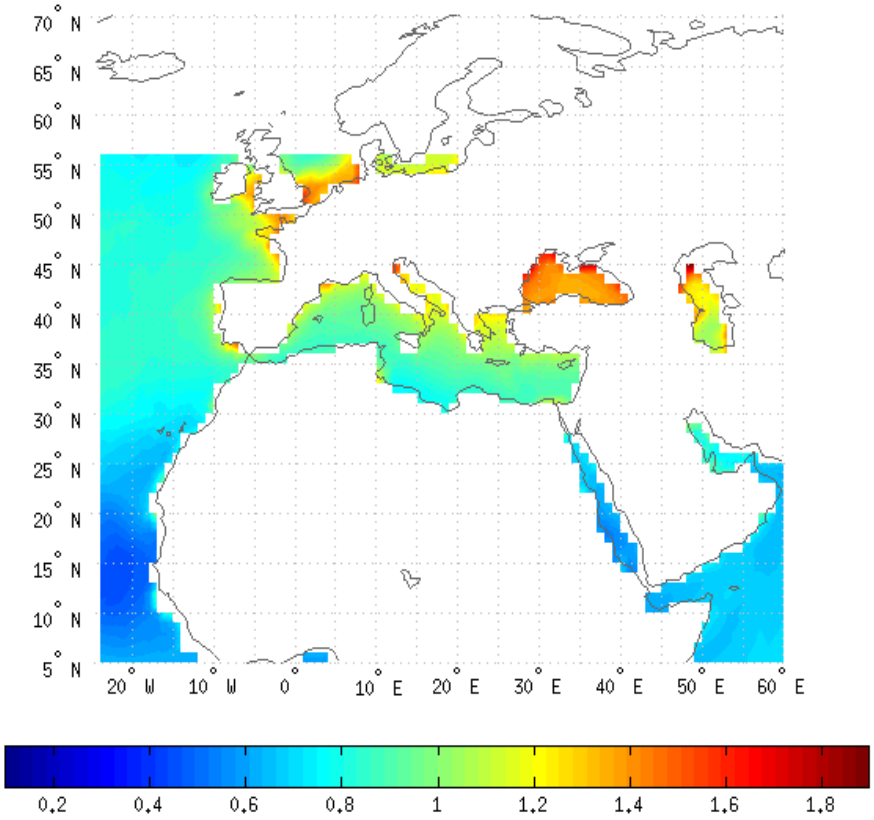

Figure 2. MODIS C006 Angström exponent at 550-865 nm for the period 2002-2010.

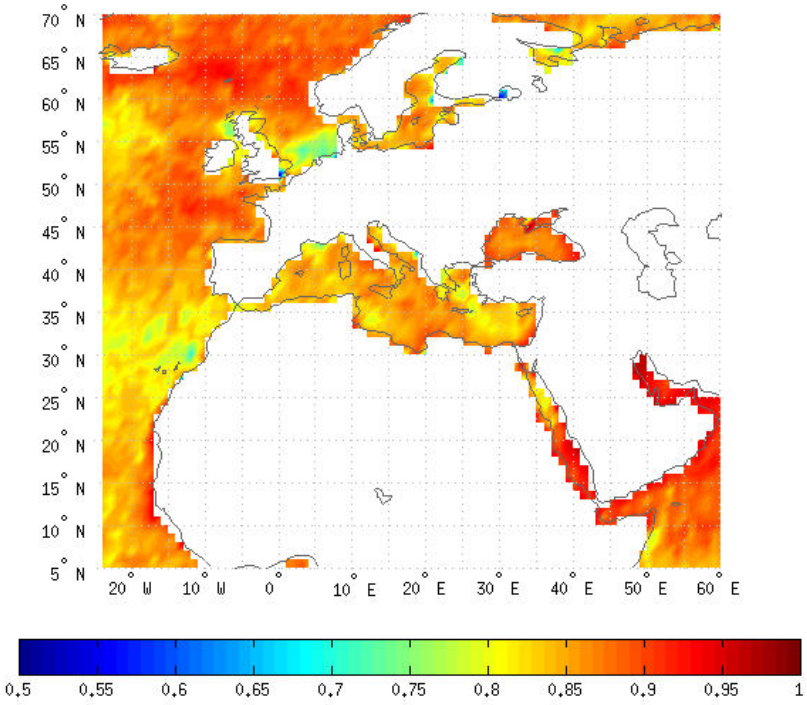

Figure 3. Correlation coefficient values between MODIS C005 and C006 Angström exponent data at 550-865 nm over the period 2002-2010.

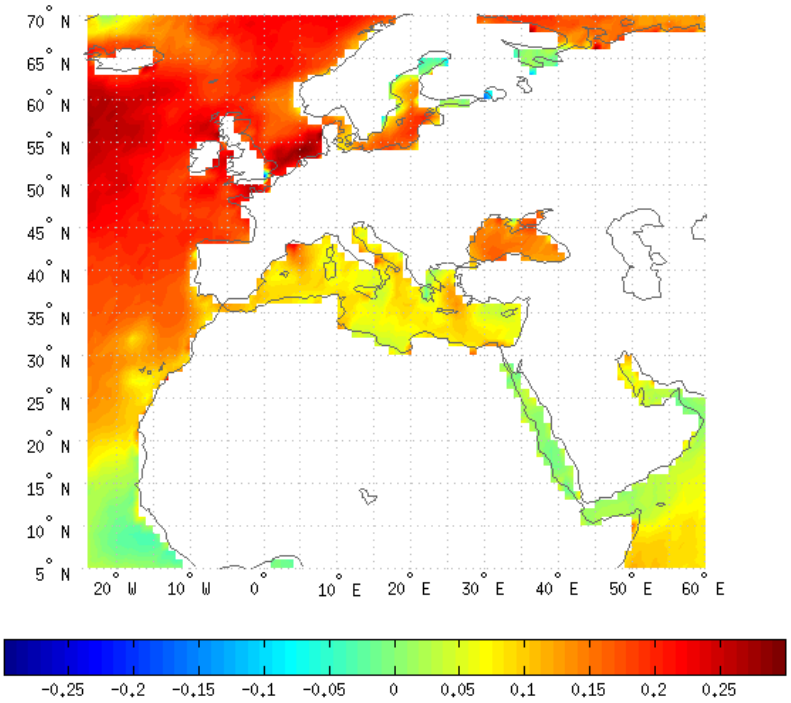

Figure 4. Biases between MODIS C005 and C006 Angström exponent data at 550-865 nm over the period 2002-2010.

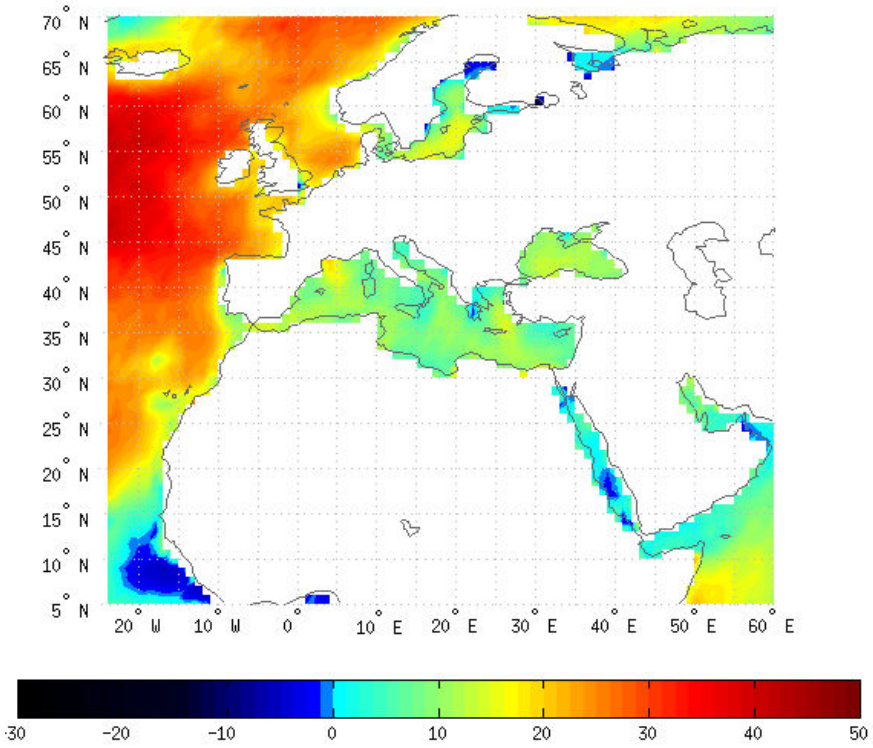

Figure 5. Percent (%) biases between MODIS C005 and C006 Angström exponent data at 550-865 nm over the period 2002-2010.

In a next step, we attempted to compare the computed trends of C005 and C006 AE data over the common period 2002-2010 in order to assess whether changes are detected, which (as

stated above and by A. M. Sayer) could be an indication of possible changes in corresponding asymmetry parameter trends. Below, in Figure 6, we show the computed deseasonalized trends of slope values for both C005 and C006.

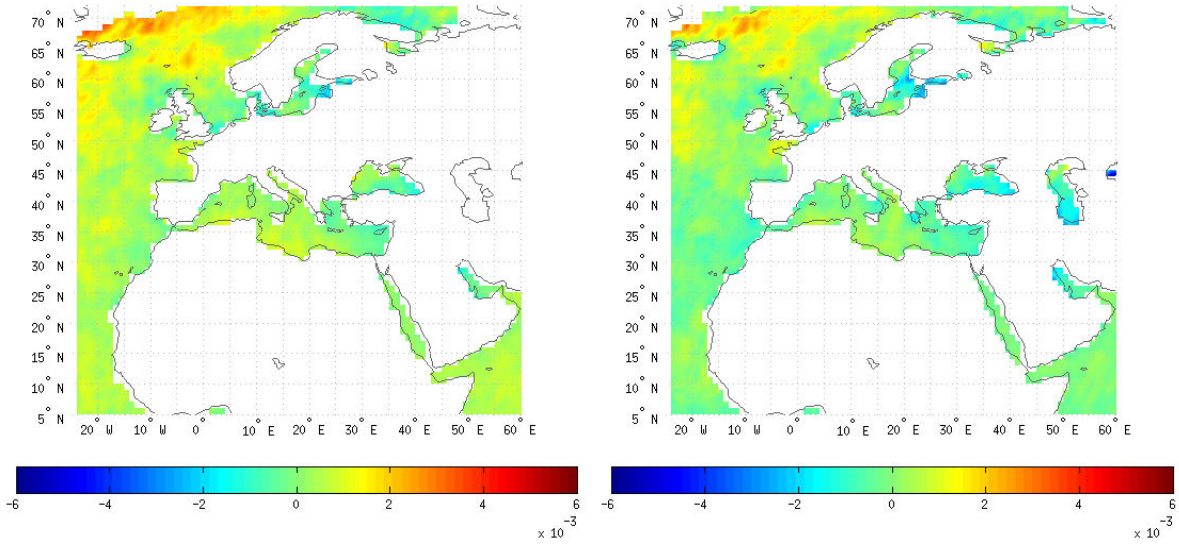

(a) (b)

Figure 6. Computed deseasonalized trends of (a) MODIS Aqua C005 and (b) C006 Angström exponent (550-865 nm) slope values for years 2002-2010.

The results reveal similar patterns again between C005 and C006. First of all, small trends are found in both of them, in agreement with the small trends of asymmetry parameter reported in our paper (sect. 3.2.2, line 354). Then, it is obvious that the sign of AE trends mainly does not change from C005 to C006. This might be a signal that no changes of aerosol asymmetry parameter are expected in C006. Although this cannot be certified, unfortunately, due to the unavailability of asymmetry parameter in C006, it puts some confidence on the C005 results given in our paper. A short note relevant to the performed analysis has been made in sect. 3.2.2, lines 373-378, whereas the results are more extensively presented in a new section 2.3.3 introduced in the revised manuscript.

- I also would not place much importance on correlation coefficient between asymmetry parameter from MODIS and AERONET. The data range is quite small and the uncertainties on both datasets (AERONET too) can be non-negligible in this case. So I would not expect a high degree of correlation. I think bias and RMS are probably more useful metrics to emphasise.

We can understand the worries of A. M. Sayer regarding the comparison between MODIS and AERONET asymmetry parameter, especially as to the use of correlation coefficient as a metric. Nevertheless, we would like to note that what may be problematic is not the small asymmetry parameter data range per se, but the possibly large AERONET and MODIS errors compared to the data range. The range is constrained by the physical limits of the asymmetry parameter encountered in nature and deciding that it is too small is essentially accepting that meaningful validation for aerosol asymmetry parameter cannot be performed. This in our opinion is not what A. M. Sayer meant. He probably meant on the other hand, that there may be a problem with the uncertainties of both AERONET and MODIS asymmetry parameter and more specifically, with the uncertainty of the AERONET one, which is the independent

variable in our comparison. It is known that existing errors in the independent variable result in "regression dilution", i.e. underestimation of the correlation coefficient and of the regression slope. It would be possible to account for this underestimation by using Deming regression, if we had an estimate of the standard error of both sensors. In its absence, R and slope values have to be left uncorrected, while mentioning that their true values are actually larger than the ones reported in the paper.

Finally, we would like to note that we consider that the comparison shown in Fig. 9 (Figure 7 of original manuscript) can be still taken as a valid predictive model, which given a measured value of g_{aer} from AERONET can predict with 95% confidence where the respective MODIS value falls (based on the definition of the prediction bands). These bands are now shown in Fig. 9.

Relevant notes to the above issue were made in the revised paper (sect. 4, lines 478-492). Moreover, taking into account the comment of A. M. Sayer, we toned down the importance of correlation coefficient, giving more emphasis in the discussion on biases and RMSE values.

References

Levy, R. C., Remer, L. A., Kleidman, R. G., Mattoo, S., Ichoku, C., Kahn, R., and Eck, T. F.: Global evaluation of the Collection 5 MODIS dark-target aerosol products over land, Atmos. Chem. Phys., 10, 10399-10420, doi:10.5194/acp-10-10399-2010, 2010.

Levy, R. C., Mattoo, S., Munchak, L. A., Remer, L. A., Sayer, A. M., Patadia, F., and Hsu, N. C.: The Collection 6 MODIS aerosol products over land and ocean, Atmos. Meas. Tech., 6, 2989-3034, doi:10.5194/amt-6-2989-2013, 2013.

Lyapustin, A., Wang, Y., Xiong, X., Meister, G., Platnick, S., Levy, R., Franz, B., Korkin, S., Hilker, T., Tucker, J., Hall, F., Sellers, P., Wu, A., and Angal, A.: Scientific impact of MODIS C5 calibration degradation and C6+ improvements, Atmos. Meas. Tech., 7, 4353-4365, doi:10.5194/amt-7-4353-2014, 2014.

Response to Reviewer 1

We would like to thank the Reviewer for his comments. We have tried to take them into account and to address the raised issues trying to provide necessary clarifications and improvements. Below are given point by point answers to the comments (also provided in Italics).

- The paper presents a short analysis of the aerosol asymmetry parameter derived from the MODIS radiometer on TERRA and AQUA satellites. The authors focus on some specific areas of the world: North Africa, Europe and the Middle East. They use the collection 5 of MODIS atmospheric products. The asymmetry parameter is retrieved only over ocean surfaces. The paper presents a validation of the MODIS asymmetry parameter with AERONET retrievals. The seasonal and interannual variability for each area is discussed.

Major remarks:

- The introduction is not appropriate. You should introduce the asymmetry parameter in a more general way including its definition and how it depends on the aerosol physical and chemical properties.

Asymmetry parameter is a common term and important parameter in radiative transfer. This is why we avoided referring to its definition and emphasized its spatial and temporal characteristics and comparison against AERONET. In response to the Reviewer request, we inserted in the revised paper a short definition and discussion of its dependency and importance. However, we preferred to do this in section 2 (Data) and not in the Introduction. Hence, at the beginning of sect. 2 the definition and a discussion on aerosol asymmetry parameter are now provided (lines 94-116).

- I would like to have a more qualitative (scientific) presentation of the optical properties you are studying.

Please note that there is only one optical property addressed in the present work. We are not sure to what the Referee refers by "… more qualitative (scientific) presentation". We believe that such a qualitative presentation of asymmetry parameter, apart from its definition and basic discussion of its dependence that has now been given, would be beyond the scope of this scientific paper. The significance and radiative effects of properties like the asymmetry parameter are very thoroughly and fittingly explained in textbooks.

- Avoid awkward sentences like "AOD (...) provides a good measure of the aerosol load over an area".

The notion that AOD is a measure of aerosol load is very widespread. All Referees of this manuscript use in their reviews the paper by Levy et al. (2010), who also embrace this description of AOD, as do also many other research papers and other scientific documents dealing with aerosols.

- A presentation of the retrieval algorithm should be given in details (method, aerosol models used, accuracy…) because you use a parameter that is not the result of the inversion procedure but is rather a by-product of the inversion.

Indeed, the aerosol asymmetry parameter is not a direct product of the MODIS inversion procedure. However, providing a description of the method, aerosol models used, accuracy etc. is beyond the scope of this study, which does not tackle with issues related to its

derivation procedure. More important, such issues and studies are addressed in more appropriate journals like the Atmospheric Measurement Techniques (AMT).

- The reason why you analyze the data only over a part of the world is unclear. MODIS data are global, AERONET data are global and the paper could be global.

The paper could truly be global, and this claim could exist for all published regional studies. However, this may produce presentation and clarity problems for physical quantities having geographically distinct and varying behavior. Such a quantity is the asymmetry parameter. For example, the paper by Levy et al. (2013) used by all Referees, reads: "MODIS/AERONET "comparability" (regression slope, intercept, correlation and number within EE envelope) varied as a function of location and season...". There is a valid reason why many regional studies from global datasets are being published. Moreover, this study complements many others of our group (e.g. Papadimas et al., 2008; Hatzianastassiou et al., 2009; Gkikas et al., 2009; 2013) dealing with other aerosol optical properties for this specific world region.

- The validation exercise is not convincing. You have a small range of asymmetry parameter and a linear model is not appropriate.

We would like to note that what may be problematic is not the small asymmetry parameter data range per se, but the possibly large AERONET and MODIS errors compared to the data range. The range is constrained by the physical limits of the asymmetry parameter encountered in nature and deciding that it is too small is essentially accepting that meaningful validation for aerosol asymmetry parameter cannot be performed. This in our opinion is not what A. M. Sayer meant. He probably meant on the other hand, that there may be a problem with the uncertainties of both AERONET and MODIS asymmetry parameter and more specifically, with the uncertainty of the AERONET one, which is the independent variable in our comparison. It is known that existing errors in the independent variable result in "regression dilution", i.e. underestimation of the correlation coefficient and of the regression slope. It would be possible to account for this underestimation by using Deming regression, if we had an estimate of the standard error of both sensors. In its absence, R and slope values have to be left uncorrected, while mentioning that their true values are actually larger than the ones reported in the paper.

Finally, we would like to note that we consider that the comparison shown in Fig. 7 can be still taken as a valid predictive model, which given a measured value of g_{aer} from AERONET can predict with 95% confidence where the respective MODIS value falls (based on the definition of the prediction bands). These bands are now shown in Fig. 9 (Fig. 7 in original ACPD manuscript).

Relevant notes to the above issue were made in the revised paper (sect. 4, lines 478-492).

- The difference between AQUA and TERRA platforms as well as the long-term analysis should include the calibration and inter-calibration issues (see Short Comment).

We acknowledge that, as extensively indicated by A. M. Sayer, there are calibration issues affecting the analysis on long-term changes of aerosol asymmetry parameter (Fig. 5, section 3.2.2). In the revised paper, reference is made to this issue (sect. 3.2.2, lines 366-377), especially in the framework of providing an explanatory factor for the detected differences in Terra and Aqua aerosol asymmetry parameter. Moreover, we have performed a detailed additional analysis using another aerosol size parameter, i.e. Angström exponent, which largely supports the findings of the present study based on asymmetry parameter. For the sake of brevity, we avoid to place here the results of this analysis, which are thoroughly presented

in the response to A. M. Sayer. We also introduced a new sub-section in the revised paper, sect. 3.2.3 named "Possible uncertainties of MODIS aerosol asymmetry parameter" has been introduced in the revised paper, where the raised important concerns of the Referee-1 (and also of the other Referee and A. M. Sayer) are fully addressed and discussed.

- Finally, the analysis of the asymmetry parameter alone doesn't provide a lot of information on the aerosol impact on radiation. The paper will be greatly improved by putting the study in a more general context including optical and microphysical properties of atmospheric aerosols.

Of course, it was not the goal of the present study to study aerosol radiative effects. Our group has performed a number of such studies dealing with the aerosol impacts on radiation either on global or regional scale (e.g. Hatzianastassiou et al., 2004a; 2004b; 2007a; 2007b; Papadimas et al. 2012). On the contrary, as clearly defined already in the Introduction, the purpose of this study is to assess the first real satellite (MODIS) based data on asymmetry parameter, which is one of the key optical properties that determine aerosol radiative effects. Such data are highly required for use in radiative transfer models, like the one used in our previously reported studies. Nevertheless, and this is a strong priority in model studies, before using input data in models it is imperative to assess its quality, and this is usually performed through comparison against surface based data.

Furthermore, we would like to note that, as shown in the present study, already performing an analysis on a single aerosol optical parameter, like the aerosol asymmetry parameter here, requires a lot of work and space for presentation. Including more parameters, optical or microphysical, would enhance the volume of obtained results which could not fit in a single paper presentation.

References

Gkikas, A., Hatzianastassiou, N., and Mihalopoulos, N.: Aerosol events in the broader Mediterranean basin based on 7-year (2000–2007) MODIS C005 data, Ann. Geophys., 27, 3509–3522, doi:10.5194/angeo-27-3509-2009, 2009.

Gkikas, A., Hatzianastassiou, N., Mihalopoulos, N., Katsoulis, V., Kazadzis, S., Pey, J., Querol, X., and Torres, O.: The regime of intense desert dust episodes in the Mediterranean based on contemporary satellite observations and ground measurements, Atmos. Chem. Phys., 13, 12135-12154, doi:10.5194/acp-13-12135-2013, 2013.

Hatzianastassiou, N.; Katsoulis, B.; Vardavas, I.. Global distribution of aerosol direct radiative forcing in the ultraviolet and visible arising under clear skies, Tellus B**,** 56, 51-71, DOI: 10.1111/j.1600-0889.2004.00085.x, 2004a.

Hatzianastassiou, N., B. Katsoulis, I. Vardavas: Sensitivity analysis of aerosol direct radiative forcing in ultraviolet - visible wavelengths and consequences for the heat budget, Tellus B, 56b, 368 - 381, 2004b.

Hatzianastassiou, N., Matsoukas, C., Drakakis, E., Stackhouse Jr., P. W., Koepke, P., Fotiadi, A., Pavlakis, K. G., and Vardavas, I.: The direct effect of aerosols on solar radiation based on satellite observations, reanalysis datasets, and spectral aerosol optical properties from Global Aerosol Data Set (GADS), Atmos. Chem. Phys., 7, 2585-2599, doi:10.5194/acp-7-2585-2007, 2007a.

Hatzianastassiou, N., Matsoukas, C., Fotiadi, A., P. W. Stackhouse Jr., Koepke, P., Pavlakis, K. G., and Vardavas, I.: Modelling the direct effect of aerosols in the solar near-

infrared on a planetary scale, Atmos. Chem. Phys., 7, 3211-3229, doi:10.5194/acp-7-3211-2007, 2007b.

Hatzianastassiou, N., A. Gkikas, N. Mihalopoulos, O. Torres, and B. D. Katsoulis: Natural versus anthropogenic aerosols in the eastern Mediterranean basin derived from multiyear TOMS and MODIS satellite data, J. Geophys. Res., 114, D24202, doi:10.1029/2009JD011982, 2009.

Levy, R. C., Remer, L. A., Kleidman, R. G., Mattoo, S., Ichoku, C., Kahn, R., and Eck, T. F.: Global evaluation of the Collection 5 MODIS dark-target aerosol products over land, Atmos. Chem. Phys., 10, 10399-10420, doi:10.5194/acp-10-10399-2010, 2010.

Levy, R. C., Mattoo, S., Munchak, L. A., Remer, L. A., Sayer, A. M., Patadia, F., and Hsu, N. C.: The Collection 6 MODIS aerosol products over land and ocean, Atmos. Meas. Tech., 6, 2989-3034, doi:10.5194/amt-6-2989-2013, 2013.

Papadimas, C. D., N. Hatzianastassiou, N. Mihalopoulos, X. Querol, and I. Vardavas: Spatial and temporal variability in aerosol properties over the Mediterranean basin based on 6-year (2000–2006) MODIS data, J. Geophys. Res., 113, D11205, doi:10.1029/2007JD009189, 2008.

Papadimas, C. D., Hatzianastassiou, N., Matsoukas, C., Kanakidou, M., Mihalopoulos, N., and Vardavas, I.: The direct effect of aerosols on solar radiation over the broader Mediterranean basin, Atmos. Chem. Phys., 12, 7165-7185, doi:10.5194/acp-12-7165-2012, 2012.

Response to Reviewer 2

We would like to thank the Reviewer for his comments, which are to a large extent similar to those of A. M. Sayer and also partly to Reviewer's 1. We took them into account and revised accordingly our paper, addressing his raised issues and concerns, and providing necessary clarifications and improvements. Below are given point by point answers to the comments (also provided in Italics).

- Having carefully read through the articles of Lyapoustin et al. 2014 and Levy et al., 2010; 2013, it comes out that even if there is no direct reference to the asymmetry parameter, the corrections needed for critical parameters in C5 data that are used to estimate the asymmetry parameter, are crucial for extracting a product trustful for interpreting its long term variability and characteristics.
Given the uncertainty of the aerosol asymmetry parameter from both datasets (MODIS and AERONET), even the evaluation via differences that may be well covered by the uncertainties, might be somewhat meaningless. Thus, a great part of the analyses presented in this paper is doubtful regarding the extent into which results reflect physical processes and trends rather than other artifacts.

The concern of the Referee about the validity of the presented asymmetry parameter (g_{aer}) results in our paper, which is also based and in line with the concerns of A. M. Sayer, has been seriously taken into account.

We would like to emphasize the importance of the existence of such a dataset, providing this important aerosol optical property to the scientific community, and to stress that, as explained in our paper, it is along with the aerosol optical depth and single scattering albedo, crucial to radiative transfer and many climate models. Therefore, it is really worth to try to assess its validity in order to ensure its quality and possible use in these models.

Therefore, we addressed in the revised manuscript the concern of the Referee in two ways:

(i) first, we also used another basic aerosol size parameter, which is well tested, the MODIS Aqua C005 Angström exponent at the 550-865 wavelength pair ($AE_{550\text{-}865}$) and compared the asymmetry parameter with it, in order to examine whether they agree or not.

(ii) Second, in order to address concerns about long-term changes related to calibration issues, we also used the more recent available MODIS Aqua Collection 006 $AE_{550\text{-}865}$ data and compared them with the corresponding C005 ones.

In both cases, a good agreement has been found, which is encouraging and puts confidence on the presented results of MODIS C005 g_{aer}.

Figure 1a displays the geographical distribution of $AE_{550\text{-}865}$ for the study period, i.e. 2002-2010. The main geographical patterns in Fig. 1a are in line with those of asymmetry parameter (Fig. 2 of ACPD paper). For example, note the high AE values in the Black Sea (yellowish-reddish colors), indicative of fine aerosols, the relatively high values in the Mediterranean Sea (greenish-yellowish colors) and the low values (deep bluish colors) off the western African coasts corresponding to exported Saharan dust. The consistency between g_{aer} and AE data is shown by the strong anti-correlation between the MODIS $AE_{550\text{-}865}$ and g_{aer} data at 660 and 870 nm, shown in Figures 1b and 1c, respectively. Strong negative correlation coefficients, larger than 0.7 and 0.8 in Figs 1a and 1b, respectively, relate inversely high/low g_{aer} values with low/high AE ones over the same areas. These results indicate that the spatial

patterns of MODIS C005 g_{aer} product are reasonable as compared to the C005 Angström exponent data.

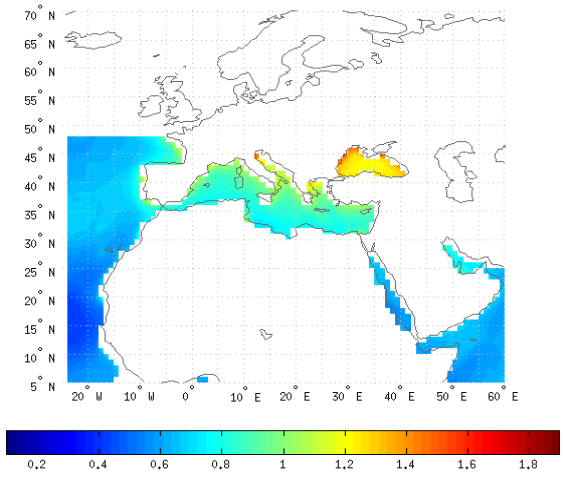

(a)

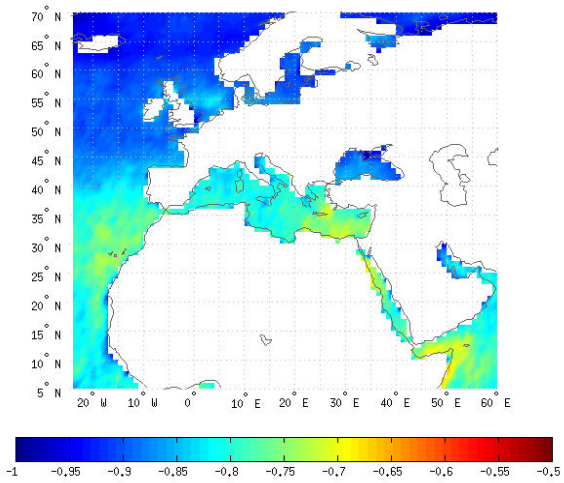

(b)

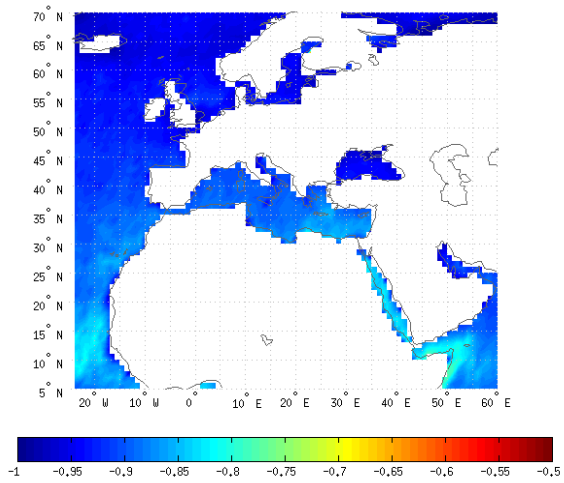

(c)

Figure 1. Geographical distribution of MODIS-Aqua C005 Angström exponent ($AE_{565\text{-}870}$) values averaged over 2002-2010, at the wavelength pair of 550-865 nm. The correlation coefficients between $AE_{550\text{-}865}$ and g_{aer} data at 660 and 870 nm are given in (b) and (c), respectively.

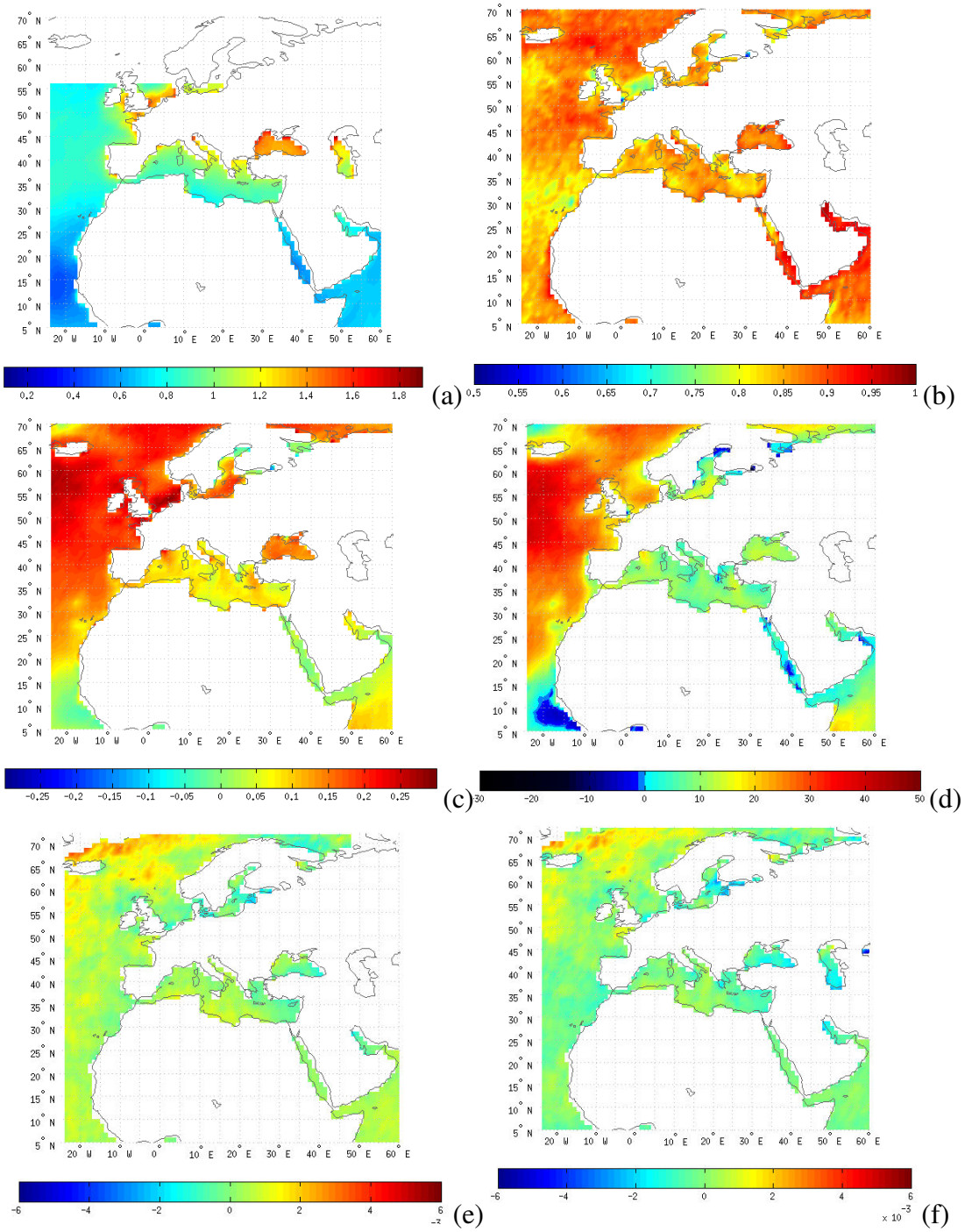

Figure 2. Geographical distribution of MODIS-Aqua C006 Angström exponent ($AE_{565\text{-}870}$) values averaged over 2002-2010, at the wavelength pair of 550-865 nm. In (b), (c) and (d) are given the correlation coefficients, the absolute biases and the relative percent biases, respectively, between the C006 and corresponding C005 $AE_{550\text{-}865}$ data. In (e) and (f) are given the computed deseasonalized trends of MODIS Aqua C005 and C006 $AE_{550\text{-}865}$) slope values for years 2002-2010, respectively.

As for the Referee's questions about possible uncertainties regarding the long-term variability of MODIS C005 aerosol size products, due to the calibration issues discussed in the previous section, the corresponding MODIS C006 AE product was also used and it is displayed in Fig.

2a. From Figs. 2a and 1a, a similarity is apparent in the main geographical patterns of the two collections' AE product. The similarity between C005 and C006 AE data is also depicted in the computed correlation coefficients (Fig. 2b), exceeding 0.8, and biases (in absolute and relative percentage terms, Figs 2c and 2d, respectively) which are smaller than 0.1 or 10% in most areas of the study region and 0.2 or 20% almost everywhere. It should be noticed that our AE results are in line with those of Levy et al. (2013, Fig. 15) which refer, however, only to year 2008 (ours are for 2002-2010). In addition, a comparison is attempted in Figs 2e and 2f between the computed trends of C005 and C006 AE data over the common period 2002-2010, in order to assess whether changes are detected, which could be an indication of possible changes in corresponding asymmetry parameter trends. Figures 2e and 2f show the computed deseasonalized trends of slope values for both C005 and C006 AE. The results reveal similar patterns between C005 and C006. Small trends are found in both of them, in agreement with the small trends of asymmetry parameter reported in the ACPD paper's Fig. 5. It is found that the sign of AE trends mainly does not change from C005 to C006. This might be a signal that no changes of aerosol asymmetry parameter are expected in C006. Unfortunately, this cannot be certified presently, due to the current unavailability of asymmetry parameter in the recently released MODIS C006 dataset. However, the similarities between C005 and C005 AE data, puts some confidence on the C005 results given in the present paper.

A new sub-section (3.2.3) named as "Possible uncertainties of MODIS aerosol asymmetry parameter" has been introduced in the revised paper, where the raised important concerns of the Referee-2 (and also of the other Referee and A. M. Sayer) are fully addressed and discussed.

- Overall, I get the impression that this work is one step behind, which is partly understandable since progress in corrections and evaluations are rapid. However, still great parts of the paper are quite descriptive and no insight is provided on the new information that might be provided from this parameter (alone but also in conjunction with other parameters not addressed at all in this paper).

We are sorry but we are not sure to what the Referee refers by "… this work is one step behind …". As for the Referee's phrase "…which is partly understandable since progress in corrections and evaluations are rapid …" we believe that it is addressed in the revised manuscript by the use of the most recent C006 MODIS Angström exponent data, which show a general nice agreement with the corresponding C005 one both in terms of spatial patterns and temporal trends (this is discussed in the previous point and in the new section 3.2.3 of the revised paper). Finally, as to the phrase "…still great parts of the paper are quite descriptive and no insight is provided on the new information that might be provided from this parameter (alone but also in conjunction with other parameters not addressed at all in this paper) …" we cannot understand to what the "new information" refers to. Features of satellite based aerosol asymmetry parameter (from MODIS) are presented for the first time to our knowledge in the literature, therefore the provided information is unprecedented and, as shown in this paper, reasonable and useful for use in radiative transfer and climate models, to which is very important. Already, the assessment of asymmetry parameter alone has obviously resulted in our long present analysis and paper. Adding more parameters would make difficult to present together their information along with g_{aer}, which is already very important by itself.

- Statements in the summary and conclusions section like "The results are consistent with the theory and thus prove a good performance of the MODIS retrieval ..." and "The identified weaknesses may provide an opportunity to improve such satellite retrievals of aerosol

asymmetry parameter in forthcoming data products like those of MODIS C006" probably support the points I am trying to raise.

We believe that the presented results and analysis in the revised version of the paper now support the statements made in the Conclusions reported by the Referee.

References

Levy, R. C., Mattoo, S., Munchak, L. A., Remer, L. A., Sayer, A. M., Patadia, F., and Hsu, N. C.: The Collection 6 MODIS aerosol products over land and ocean, Atmos. Meas. Tech., 6, 2989-3034, doi:10.5194/amt-6-2989-2013, 2013.

The regime of aerosol asymmetry parameter over Europe, Mediterranean and Middle East based on MODIS satellite data: evaluation against surface AERONET measurements

M. Korras Carracca[1], N. Hatzianastassiou[2,*], C. Matsoukas[1], A. Gkikas[2], C. D. Papadimas[2]

[1]{ Department of Environment, University of the Aegean, 81100 Mytilene, Greece}

[2]{ Laboratory of Meteorology, Department of Physics, University of Ioannina, 45110 Ioannina, Greece}

Correspondence to: N. Hatzianastassiou (nhatzian@cc.uoi.gr)

Abstract

Atmospheric particulates are a significant forcing agent for the radiative energy budget of the Earth-atmosphere system. The particulates' interaction with radiation, which defines their climate effect, is strongly dependent on their optical properties. In the present work, we study one of the most important optical properties of aerosols, the asymmetry parameter (g_{aer}), in the region comprising of North Africa, the Arabian peninsula, Europe, and the Mediterranean basin. These areas are of great interest, because of the variety of aerosol types they host, both anthropogenic and natural. Using satellite data from the collection 051 of MODIS (MODerate resolution Imaging Spectroradiometer, Terra and Aqua), we investigate the spatio-temporal characteristics of the asymmetry parameter. We generally find significant spatial variability, with larger values over regions dominated by larger size particles, e.g. outside the Atlantic coasts of north-western Africa, where desert-dust outflow is taking place. The g_{aer} values tend to decrease with increasing wavelength, especially over areas dominated by small particulates. The intra-annual variability is found to be small in desert-dust areas, with maximum values during summer, while in all other areas larger values are reported during the cold season and smaller during the warm. Significant intra-annual and inter-annual variability is observed around the Black Sea. However, the inter-annual trends of g_{aer} are found to be generally small.

Although satellite data have the advantage of broad geographical coverage, they have to be validated against reliable surface measurements. Therefore, we compare satellite-measured values with g_{aer} values measured at 69 stations of the global surface AERONET (Aerosol Robotic Network), located within our region of interest. This way, we provide some insight on the quality and reliability of MODIS data. We report generally better agreement at the wavelength of 870 nm (correlation coefficient R up to 0.47), while of all wavelengths the results of the comparison were better for spring and summer.

1 Introduction

Atmospheric aerosol particles interact with radiation, mainly the short wave (SW or solar) part of the spectrum, modifying the energy budget of the Earth-atmosphere system. The aerosol effect is either direct, through the scattering and absorption of solar radiation, and thus reducing the incoming solar radiation flux at the surface, indirect, through the modification of cloud properties, or semi-direct, due to the absorption of solar radiation and consequent modification of the atmospheric temperature profile, convection, and cloud properties (e.g. Graβl, 1979; Hansen, 1997; Lohmann and Feichter, 2005).

The interaction of particles with the solar flux, which defines their climate role, strongly depends on their optical properties (Hatzianastassiou et al., 2004; 2007), which cannot be covered globally by surface in situ measurements. Besides the aerosol optical depth (AOD), which provides a good measure of the aerosol load over an area, one of the most important optical properties of atmospheric particles, which is used in radiative transfer, climate, and general circulation models, is the asymmetry parameter (g_{aer}). The asymmetry parameter describes the angular distribution of the scattered radiation and determines whether the particles scatter radiation preferentially to the front or back. The globally available satellite based AOD data are considered to a great extent reliable and adequate, due to significant developments in surface and satellite measurements during the last two decades, and particularly after 2000. On the other hand, despite of the important role of the asymmetry parameter, relevant global coverage data are measured only for the few last years, or are available in long-term aerosol climatologies such as Global Aerosol Data Set (GADS, Koepke et al. 1997) and Max Planck Aerosol Climatology (MAC, Kinne et al., 2013). Even so, asymmetry parameter data are usually examined for regions with limited geographical

extent and temporal coverage (Di Iorio et al, 2003), without intercomparison between alternative data platforms.

The goal of the present work is the study of the spatiotemporal distribution of the aerosol asymmetry parameter, using the most recent data from MODIS (MODerate resolution Imaging Spectroradiometer, collection 051). Emphasis is given to the comparison between the provided MODIS data and respective reliable surface measurements of the global AERONET, in order to gain insight on the quality of the former.

For this study we focus on the region defined by latitudes 5°N to 70°N and longitudes 25°W to 60°E, including North Africa, the Arabian peninsula, Europe, and the greater Mediterranean basin (Fig. 1). This area is selected because of the simultaneous presence of a variety of particles, both natural and anthropogenic (e.g. desert dust, marine, biomass burning, anthropogenic urban / industrial pollution) as shown in previous studies (Lelieveld et al., 2002; Sciare et al., 2003; Pace et al., 2006; Lyamani et al., 2006; Gerasopoulos et al., 2006; Kalivitis et al., 2007). This is due to the fact that two of the largest deserts of the planet are partly included in our area of interest, i.e. the Arabian desert and the Sahara, while one finds also significant sources of anthropogenic pollution, mainly in the European continent, with urban and industrial centres. Moreover, our area of interest and primarily its desert areas, are characterised by a large aerosol load (large optical depth, Remer et al. 2008). Finally, significant regions in this area, more specifically the Mediterranean basin and North Africa, are considered climatically sensitive, since they are threatened by desertification (IPCC, 2007; 2013). This is the first study (to our knowledge) that focuses on asymmetry parameter over a geographically extended area, while at the same time compares satellite with ground-station data.

2 Data

Before presenting the data used in this study a short introduction of the parameter studied is given here for readers more or less unfamiliar with it. The asymmetry parameter (or factor) is defined by:

$$g = \frac{\overline{\omega}_1}{3} = \frac{1}{2}\int_{-1}^{1} P(\cos\Theta)\cos\Theta d\cos\Theta \qquad (1)$$

where P is the phase function, which represents the angular distribution of the scattered energy as a function of the scattering angle Θ and it is defined for molecules, cloud particles, and aerosols, namely our study case. The phase function can be expressed using the Legendre polynomials $\overline{\omega}_l$ (see Liou, 2002) and $\overline{\omega}_1$ in Eq. (1) stands for l=1. The asymmetry parameter is the first moment of the phase function and it is an important parameter in radiative transfer. For isotropic scattering, g equals zero, which is the case for Rayleigh molecular scattering. The asymmetry parameter increases as the diffraction peak of the phase function sharpens. For Lorenz-Mie type particles, namely for aerosols and cloud droplets, the asymmetry parameter takes positive values denoting a relative strength of forward scattering, with increasing values with increasing particle size. It can also take negative values if the phase function peaks in backward directions (90-180°). The phase function along with the extinction coefficient (or equivalently the optical depth) and the single scattering albedo, constitute the fundamental parameters that drive the transfer of diffuse intensity. The asymmetry parameter itself is a simple expression of the phase function (being its first moment) and it is used in many radiative transfer and climate models. Hence, the importance of aerosol asymmetry parameter is easily understood for enabling computations of aerosol radiative properties and effects (e.g. forcings).

Daily data of the aerosol asymmetry parameter (g_{aer}) are used for the needs of this work. In order to achieve the largest geographical coverage of the studied region, we employ satellite data from the MODIS-Terra and MODIS-Aqua datasets. These data are compared with in-situ measurements at stations of the AERONET. We provide a detailed description of the utilised data in the following sections.

2.1 Satellite MODIS Terra and Aqua data

MODIS is an instrument (radiometer) placed on the polar-orbiting satellites of NASA (National Aeronautics and Space Administration) Terra and Aqua, 705 km from the Earth, in the framework of the Earth Observing System (EOS) programme. Terra was launched on 18 December 1999, while Aqua was launched on 4 May 2002. The two satellites are moving on opposite directions and their equatorial crossing times are at 10:30 (Terra) and 13:30 (Aqua). MODIS is recording data in 36 spectral channels between the visible and the thermal infrared (0.44 – 15 μm), while its swath width is of the order of 2330 km, which results in almost full planetary coverage on a daily

132 basis. The global MODIS database is generally considered as one of the most reliable
133 at present.

134 Aerosol properties are monitored in 7 spectral channels between 0.47 and 2.13 μm
135 and final results are derived through algorithms developed for aerosol quantities both
136 over land and ocean (Kaufman et al., 1997; Tanré et al., 1997; Ichoku et al., 2002;
137 Remer et al., 2005). MODIS data are organised in "collections" and "levels".
138 Collections comprise data produced by similar versions of the inversion algorithms,
139 with the most recent being "051", which includes also outputs from the "Deep Blue"
140 algorithm. Levels are characterised by data of different quality analysis and spatial
141 resolution.

142 In this study we use daily MODIS data for the asymmetry parameter (g_{aer}) provided
143 on an 1°x1° grid (namely 100x100 km), from the most recent Collection 051, Level
144 3. These data were measured at wavelengths 470, 660, and 870 nm, only over oceanic
145 regions, since they were derived through the algorithm for aerosol properties over the
146 ocean. The period of analysis stretches from 24-2-2000 to 22-9-2010 for MODIS-
147 Terra and from 4-7-2002 to 18-9-2010 for MODIS-Aqua. We also used Level 3 daily
148 Angström exponent data from MODIS-Aqua C005, and also spectral aerosol optical
149 depth data from MODIS-Aqua C006 datasets, from which we computed C006
150 Angström exponent. These data were used to assess the validity of g_{aer} data and their
151 changes, as discussed in section 3.2.3.
152

153 **2.2 Ground based AERONET data**

154 AERONET (AErosol RObotic NETwork) is a global network of stations focused on
155 the study of aerosol properties. AERONET currently encompasses about 970 surface
156 stations (number continuously evolving) equipped with sun photometers of type
157 CIMEL Electronique 318 A (Holben et al., 1998), which take spectral radiation flux
158 measurements.

159 The optical properties of aerosols are extracted through the application of inversion
160 algorithms (Dubovik and King, 2000). Data are provided on three levels (1.0, 1.5, and
161 2). In the present work, we use the most reliable Level 2 data, due to their being
162 cloud-screened and quality-assured. AERONET calculates the asymmetry parameter
163 at wavelengths 440, 675, 870, and 1020 nm. We employ daily Level 2 asymmetry
164 parameter data from 69 stations (Fig. 1), contained in our study area (N. Africa,

Arabian peninsula, Europe). We choose only coastal stations, in order to maximize the coexistence of satellite marine g_{aer} data with surface data. Also, in order to compare corresponding data between the satellite and station platforms, we perform comparison only for the 440, 675 and 870 nm.

3 Satellite based results

3.1 Geographical distributions

The spatial distribution of annual mean values of g_{aer} is given in Fig. 2 separately at the wavelengths 470, 660 and 870 nm. The values are averages over the common period between Terra and Aqua, namely 4 July 2002 till 18 September 2010. A significant spatial variability is evident, with MODIS-Terra values varying within the ranges 0.63 - 0.76, 0.57 – 0.75, and 0.55 – 0.74, at 470, 660 and 870 nm, respectively. The results exhibit a decreasing tendency of g_{aer} with increasing wavelength, consistent with the theory. Similar results are also obtained from MODIS-Aqua, but with slightly smaller values than Terra by up to 0.02 on average. More specifically, the corresponding ranges of wavelengths are 0.63 - 0.75, 0.57 – 0.73, and 0.55 – 0.73. The smaller Aqua than Terra g_{aer} values could be attributed to smaller sizes of aerosols in midday than morning, corresponding to passages of Aqua and Terra, respectively, associated with lower relative humidity values and shrinking of aerosol particles. Such diurnal variation has been also reported for AOD (Smirnov et al., 2002; Pandithurai et al., 2007), but either decreasing or increasing in the day because of the influence of other factors too, e.g. emissions or wind conditions, apart from aerosol hygroscopicity.

In general, the largest g_{aer} values (deep red colors) are observed off the coasts of West Africa (eastern tropical Atlantic Ocean) at all three wavelengths. High values are also found over the Red and Arabian Seas. These high values are due to strong dust outflows from the Saharan and Arabian deserts carrying out coarse aerosol particles causing strong forward scattering. Nevertheless, the Persian Gulf region, which is surrounded by deserts, is characterized by relatively smaller g_{aer} values. More specifically, values as small as 0.69 (MODIS-Terra) and 0.67 (MODIS-Aqua) are observed in this region at 470 nm, while at the longer wavelengths (660, 870 nm) the smallest values are equal to 0.66 (Terra) and 0.64 (Aqua). The smaller g_{aer} values over the Persian Gulf can be attributed to the presence of fine aerosols, which is

corroborated by the low effective radius and large fine-fraction measurements by MODIS over the Persian Gulf, compared to neighbouring areas (not shown here). These fine particles originate from the industrial activities in the Gulf countries related to oilfields or refineries (Goloub and Arino, 2000; Smirnov et al., 2002a,b; Dubovik et al., 2002).

The high g_{aer} values over the northeastern tropical Atlantic Ocean as well as west of the Iberian coasts are possibly related with the presence of coarse sea salt particles. On the other hand, the asymmetry parameter takes clearly smaller values over the Black Sea, where according to MODIS-Terra varies between 0.63 and 0.7 at 470 nm, 0.57 and 0.67 at 660nm, and 0.55 and 0.66 at 870 nm, with the smallest values appearing in the Crimean peninsula (corresponding maximum Aqua values are smaller by 0.02). The small Black Sea g_{aer} values can be associated with the vicinity of industrial but also biomass burning activities in nearby countries. A region of special interest is the Mediterranean basin since it hosts a large variety of aerosols like anthropogenic, desert dust or sea salt (e.g. Barnaba and Gobbi, 2004). The MODIS results over this region show relatively small g_{aer} values, secondary to those of Black Sea, characterized by an increase from north to south, which is more evident at 660 and 870 nm. More specifically, based on MODIS-Terra, g_{aer} over the Mediterranean takes values from 0.68 to 0.74 at 470 nm, while at 670 and 870 nm it ranges from 0.64 to 0.73 and 0.62 to 0.72, respectively. According to MODIS-Aqua the g_{aer} values are slightly smaller again. The observed low values in the northern parts of the Mediterranean are probably associated with the presence of fine anthropogenic aerosols transported from adjacent urban and industrial areas in the north, especially in central Europe. In contrast, the higher g_{aer} values in the southern Mediterranean, particularly near the North African coasts, can be explained by the proximity to the Sahara desert and the frequent transport of significant amounts of coarse dust (e.g. Kalivitis et al., 2006; Hatzianastassiou et al., 2009; Gkikas et al., 2009; 2014).

The spatial distributions of climatological monthly mean g_{aer} values from MODIS-Aqua at 470 nm reveal significant differences either as to the range or to the patterns of the seasonal variability, depending on the area (Fig. 3). Thus, in tropical and sub-tropical areas of Atlantic Ocean (up to about 30°N), where dust is exported from Sahara, g_{aer} keeps high values throughout the year, which reach or even exceed 0.74 locally. Over the regions of Arabian and Red Seas and the Gulf of Aden, which also experience desert dust transport, larger g_{aer} values appear in the period from March to

September, with a maximum on August (locally as high as 0.75-0.76). This seasonal behavior is in line with intra-annual changes of dust production over the Arabian peninsula indicated primarily by MODIS Angström Exponent (AE) and secondarily by Deep Blue aerosol optical depth data and reported in the literature (Prospero et al., 2002). Indeed, the production of dust there is relatively poor in winter, increases in March and April and becomes maximum in June and July (Prospero et al., 2002). Over the Arabian Sea, it is known that large amounts of desert dust are carried out during spring and early summer (Prospero et al, 2002; Savoie et al., 1987; Tindale and Pease, 1999; Satheesh et al., 1999). Nevertheless, according to MODIS, the seasonal variability of g_{aer} remains relatively small there in line with a small seasonal variability in MODIS Deep Blue AE data. This can be explained by the presence of sea salt coarse particles throughout the year, with which dust particles co-exist.

A greater seasonal variability exists over the Persian Gulf, where g_{aer} values are higher during spring and in particular in summer (up to 0.74 at 470 nm according to Aqua), and smaller in autumn and winter (area-minimum values smaller than 0.65). This seasonal behavior can be explained taking into account the meteorological conditions over the greater area of the Gulf; from June to September dry northwestern winds (Shamal) blow from northwest carrying desert dust from the arid areas of Iraq (Heishman 1999; Smirnov et al. 2002a,b). The transport of dust is gradually decreased in autumn, minimizes in winter and increases again in spring. When the presence of desert dust is limited, a significant fraction of total aerosol load in the region is consisted of fine anthropogenic particles (Smirnov et al. 2002a,b), which can explain the observed relatively small g_{aer} values in autumn and winter.

In the Mediterranean basin, g_{aer} exhibits a relatively small seasonal variation, though lower values tend to appear in summer and secondarily in early and late spring, in line with the stronger presence of dust in the area, transported from the Sahara desert (Gkikas et al., 2013). On the contrary, over the Black Sea, a clear seasonal cycle is apparent, with higher values in the cold period of the year and smaller in the warm one. More specifically, according to MODIS-Aqua, the values at 470 nm drop down to 0.61 in summer months whereas they reach 0.7 in January and December.

It is also interesting to look at the geographical distribution of monthly g_{aer} values in latitudes higher than 50°N, for which annual mean values were not given in Fig. 2 because of unavailability of data for all months. Off the coasts of northern France (English Channel) and Germany the asymmetry parameter has small values, with a

non-significant annual course (note that values do not exist for January and February). In these areas, the aerosol load consists mainly of anthropogenic polluted particles, which explains the small g_{aer} values there.

In the Baltic Sea (values available from March to October) g_{aer} shows a significant spatial and temporal variability. More specifically, it is small during summer whereas it increases, locally up to more than 0.7, in March and October. The smaller summer values can be explained by the presence of fine aerosols in the Baltic Sea originating from forest fires in Europe and Russia (Zdun et al., 2011). On the contrary, in autumn the local aerosol loading consists largely of coarse marine aerosols . It is also important to note that the Baltic Sea hosts significant amounts of anthropogenic industrial and urban aerosols throughout the year, but especially in summer (Zdun et al., 2011).

In the higher latitudes of Atlantic Ocean, where the presence of maritime aerosols is dominant, it is observed a remarkable month by month variation of asymmetry parameter, with low values in summer (values up to 0.59) against high values (up to 0.75-0.77) in spring (March, April) and autumn (October). This difference is possibly explained by the seasonal variability of aerosol size in the northern Atlantic. Apart from the presence of coarse sea salt throughout the year, in spring and summer small particles are formed through photochemical reactions of dimethylsulphide (DMS) emitted by phytoplankton decreasing the aerosol size. Moreover during summer fine anthropogenic aerosols are transported in the region from North America (Yu, 2003; Chubarova, 2009). These result in lower g_{aer} values between May and August.

Based on MODIS-Terra, the patterns of spatial distribution are generally the same with Aqua, with slightly larger g_{aer} values. At larger wavelengths (660, 870 nm) it is observed a decrease of g_{aer}, in particular of its smallest values. Further details and also an overall picture will be given later on, in the section (3.2.1) which deals with climatological monthly mean values not at the pixel but regional level.

3.2 Temporal variability

3.2.1 Seasonal variability

In order to provide an easier assessment of the seasonal cycle of aerosol asymmetry parameter and its changes from a region to another, but also among the different wavelengths (470, 660 and 870 nm), the study region was divided in 6 smaller sub-

299 regions (see Fig. 1). For each sub-region, the average values of monthly mean
300 climatological data of the pixels found within each sub-region's geographical limits
301 have been computed and are given in Fig. 4, for every wavelength and for Terra and
302 Aqua. It appears that the seasonal cycle differs between the sub-regions, as it has been
303 already shown in the geographical map distributions discussed in the previous section.

304 At 470 nm (Fig. 4i), the intra-annual variability of g_{aer} is greater over the Black Sea,
305 where it is as large as 0.06 according to MODIS-Terra and 0.05 according to MODIS-
306 Aqua, the north-eastern Atlantic Ocean (0.04 and 0.05 for Terra and Aqua,
307 respectively) and the seas of North Europe (0.05 for both Terra and Aqua). In these
308 regions, there is a tendency for smaller values during summer. More specifically, in
309 the Black Sea the smallest g_{aer} value (0.64) is observed in June, over the seas of North
310 Europe in July and over the north-eastern Atlantic Ocean in August. In these regions,
311 the largest values appear in the cold period of the year. Reverse seasonality with a
312 large seasonal amplitude is observed over the Persian Gulf, where the variability is as
313 large as 0.08, according to both MODIS-Terra and Aqua. The seasonal cycle of g_{aer}
314 over the Middle East exhibits a smaller range of variability (0.02 for MODIS-Terra
315 and 0.03 for Aqua) along with a reverse seasonal variation, with maximum values in
316 summer and minimum in winter. In the other two sub-regions (Mediterranean and
317 eastern Atlantic Ocean) the annual range of values is small (< 0.02). It is noteworthy
318 that in the Mediterranean Sea, there is a weak tendency of appearance of double
319 maxima in winter and spring. The spring maximum should be associated with the
320 presence of desert dust particles, which are transported from Sahara, mainly in the
321 eastern Mediterranean in this season (e.g. Fotiadi et al., 2006; Kalivitis et al., 2007;
322 Papadimas et al. 2008, Gkikas et al. 2009; Hatzianastassiou et al., 2009; Gkikas et al.,
323 2013). There is also a similar transport of Saharan dust in the central and western
324 Mediterranean during summer and autumn (e.g. Gkikas et al., 2009; 2013), but then
325 the predominance is not so clear because of the co-existence of fine anthropogenic
326 aerosols. Regardless of the annual cycle, smaller g_{aer} values are clearly distinguished
327 over the Black Sea and North Europe seas throughout the whole year.

328 At 660 nm, the g_{aer} values are lower than at 470 nm, in particular over Black Sea,
329 North Europe and North-East Atlantic, whereas the intra-annual variability (range of
330 g_{aer} values) increases up to 0.1 (Terra) and 0.08 (Aqua) over the Black Sea. This
331 increase is mainly attributed to the reduction of summer values due to the strong
332 appearance of fine aerosols in this season. Also, at 660 nm, there is a clearer double

annual variation of g_{aer} over the Mediterranean Sea than at 470 nm. At 870 nm the general picture is similar to that of 660 nm though a further increase of month by month variability is noticeable.

In general, our results indicate that over the regions characterized by a strong presence of desert dust particles (eastern Atlantic and the Middle East and Mediterranean Seas) the annual range of variability of g_{aer} is smaller than in the other regions. An additional feature above regions with desert dust is the smaller decrease of g_{aer} values with increasing wavelengths, which can be attributed to the different spectral behavior of solar radiation scattering by fine and coarse aerosols (e.g. Dubovik et al, 2002; J. Bi et al, 2011).

It should be noted here that according to our results, using MODIS-Terra and Aqua data, the g_{aer} seasonal cycle is about similar but with generally greater larger Terra than Aqua values.

3.2.2 Inter-annual variability and changes

Figure 5 displays the geographical distribution of the slope of inter-annual trend of g_{aer} over the study region, as computed from the application of the Mann-Kendall test to time series of deseasonalized monthly anomalies of g_{aer} at 470 nm. Results are shown in units decade^{-1} for both Terra and Aqua over their common time period, namely 2002 – 2010, only if the trend is statistically significant at the 95% confidence level. We also performed the same analysis for the 660 and 870 nm (not shown), with similar results to the 470 nm wavelength.

In general, the estimated changes are relatively small. Terra produces widely statistically significant positive trends, showing that during the period of interest, the asymmetry parameter increased over the examined area, with very few exceptions. The results from Aqua are statistically significant at considerably fewer cells, but also give a few points with decreasing g_{aer}. Based on Terra data, the stronger increases are observed in the eastern and southern Black Sea, as well as over the Baltic and Barents Seas. According to MODIS-Aqua, negative changes are found over few Atlantic Ocean cells. Both Aqua and Terra report increases of g_{aer} over the Persian Gulf, the Red Sea, South Black Sea, East Mediterranean, the coast of the Iberian Peninsula, and some coastal areas of West Africa. The differences encountered between the Terra and Aqua g_{aer} trends may be attributed to the different time of passage of each satellite platform carrying the same MODIS instrument, given that everything else is the same.

Nevertheless, most probably, they may be the result of calibration differences between the two MODIS sensors. It is known that there is a degradation of MODIS sensor (Levy et al., 2010; Lyapustin et al., 2014) impacting time series of MODIS products. More specifically, it is also known that Terra suffers more than Aqua from optical sensor degradation. These calibration issues are known to affect MODIS AOD retrievals, producing an offset between Terra and Aqua, and they are also expected to affect aerosol asymmetry parameter, which is probably more sensitive to such calibration uncertainties that AOD. In this sense, the results of Fig. 5 shown here are not to be taken as truth but rather they are given as a diagnostic of a problematic situation with MODIS aerosol asymmetry parameter inter-annual changes. Such calibration issues are expected to be addressed, at least partly, in the new Collection 006 products. Nevertheless, a preliminary comparison between MODIS Aqua C005 and C006 Angström exponent (AE), which is a common aerosol size parameter, using AE data for the 550-865 pair of wavelengths spanning the period 2002-2010, does not reveal significant modifications in geographical patterns of AE inter-annual changes. This puts some confidence on the C005 g_{aer} results given in the present study. The results of this analysis are presented in detail in the next sub-section (3.2.3).

The overall g_{aer} changes of Fig. 5 may hide smaller timescale variations of g_{aer}, which are obtained by the time-series shown in Fig. 6. Results are given for the 7 sub-regions defined previously, at the three different wavelengths and for Terra and Aqua separately. A general pattern is the decrease of g_{aer} values with increasing wavelength, in particular from 470 to 660 nm. The largest month to month and year to year variation is for Black Sea (Fig. 6i). Relatively large variability is also found in the sub-regions of NE Atlantic (6v), North Europe (6vi) and the Persian Gulf (6vii). On the contrary, small variability is noticed in the eastern Atlantic, where systematic dust outflows from Sahara take place leading to consistently high values of g_{aer}. There are also some other interesting patterns, like the significant drop of g_{aer} with wavelength in areas characterized by the presence of fine aerosols, namely the Black Sea, North Europe and the Persian Gulf (Figs, 6i,vi,vii, respectively). The specific patterns of inter-annual changes of g_{aer} are suggested by both Terra and Aqua, though a slight overestimation by Terra is again apparent in this figure. The obtained results of our analysis are meaningful and in accordance with the theory, underlining the ability of satellite observations to reasonably capture the g_{aer} regime over the studied regions.

3.2.3 Possible uncertainties of MODIS aerosol asymmetry parameter

The MODIS aerosol asymmetry parameter is not a direct retrieval product of the MODIS retrieval algorithm, but it is rather a derived by product. Since this parameter is dependent on aerosol modes used and relative weights, it is understood that there can be uncertainties associated with it. Therefore questions may arise about the validity of g_{aer} and their spatial and temporal patterns presented in the previous sub-sections. Given that, as it was already mentioned, it is an aerosol optical parameter that is valuable and highly required by radiative transfer and climate models, it is worth assessing it through comparison against another more common aerosol size parameter, namely the C005 MODIS Angström exponent at the 550-865 nm wavelength pair ($AE_{550\text{-}865}$) over ocean, which is an evaluated MODIS aerosol size product (Levy et al., 2010). Figure 7a, displays the geographical distribution of AE for the study period, i.e. 2002-2010. The main geographical patterns in Fig. 7a are in line with those of asymmetry parameter (Fig. 2). For example, note the high AE values in the Black Sea (yellowish-reddish colors), indicative of fine aerosols, the relatively high values in the Mediterranean Sea (greenish-yellowish colors) and the low values (deep bluish colors) off the western African coasts corresponding to exported Saharan dust. The consistency between g_{aer} and AE data is shown by the strong anti-correlation between the MODIS $AE_{550\text{-}865}$ and g_{aer} data at 660 and 870 nm, shown in Figures 7b and 7c, respectively. Strong negative correlation coefficients, larger than 0.7 and 0.8 in Figs 7b and 7c, respectively, relate inversely high/low g_{aer} values with low/high AE ones over the same areas. These results indicate that the spatial patterns of MODIS C005 g_{aer} product are reasonable as compared to the C005 Angström exponent data.

Since questions arise about possible uncertainties regarding the long-term variability of MODIS C005 aerosol size products, due to the calibration issues discussed in the previous section, the corresponding MODIS C006 AE product is displayed in Fig. 8a. From Figs. 8a and 7a a similarity is apparent in the main geographical patterns of the two collections' AE product. The similarity between C005 and C006 AE data is also depicted in the computed correlation coefficients (Fig. 8b), exceeding 0.8, and biases (in absolute and relative percentage terms, Figs 8c and 8d, respectively) which are smaller than 0.1 or 10% in most areas of the study region and 0.2 or 20% almost everywhere. It should be noticed that our AE results are in line with those of Levy et al. (2013, Fig. 15) which refer, however, only to year 2008 (ours are for 2002-2010). In addition, a comparison is attempted in Figs 8e and 8f between the computed trends of C005 and C006 AE data over the common period 2002-2010, in order to assess

whether changes are detected, which could be an indication of possible changes in corresponding asymmetry parameter trends. Figures 8e and 8f show the computed deseasonalized trends of slope values for both C005 and C006 AE. The results reveal similar patterns between C005 and C006. Small trends are found in both of them, in agreement with the small trends of asymmetry parameter reported in Fig. 5. It is found that the sign of AE trends mainly does not change from C005 to C006. This might be a signal that no changes of aerosol asymmetry parameter are expected in C006 and puts some confidence on the C005 results given in the present study.

4 Evaluation against AERONET data

In this section, we compare the satellite-measured aerosol asymmetry parameter with measurements from the global network of surface stations of AERONET, which is considered as the reference dataset (Holben et al., 1998). For this purpose, we identified the AERONET stations inside our area of interest and finally utilised only the coastal ones, so that both satellite and surface data be available. The total number of these stations is 69, and their locations are shown in Fig. 1 (blue squares).

Table 1 contains the comparison statistical metrics for all wavelengths (Pearson correlation coefficient, bias, standard deviation, slope, intercept) of the comparison between surface data from AERONET and satellite data from MODIS-Terra and MODIS-Aqua, which correspond to the 1°x1° cell wherein each station is located. For this analysis, we use all cells and days with common data between Terra-AERONET and Aqua-AERONET. The mean differences are calculated as g_{aer}(AERONET)-g_{aer}(Aqua) and g_{aer}(AERONET)-g_{aer}(Terra).

In general, we may note that on an annual level, the MODIS-Terra and Aqua asymmetry parameter values at 470 nm are not in very good agreement with the respective data from AERONET at 440 nm, while the results at the largest wavelengths are more reassuring, though not being very satisfactory (increasing R and decreasing relative bias and RMSE values at 675/660 nm and 870 nm). At 870 nm (Table 1 and Fig. 9), correlation coefficients are found to be the largest and equal to 0.47 (AERONET-Terra) and 0.46 (AERONET-Aqua), while satellite data are slightly overestimated compared to the surface data (bias -0.035 or 5.54% and -0.015 or -2.43%, respectively).

It is important to note that the agreement of satellite and surface data is better in spring and summer, for all studied wavelengths. Specifically, the correlation

coefficients increase up to 0.35, 0.50 and 0.54 at 440/470 nm, 660/675 nm and 870 nm, respectively, while the bias decreases down to 0.0005 (0.07%), 0.003 (0.46%) and 0.007 (1.11%), respectively.

Moreover, we find that for all seasons g_{aer} values at 870 nm and 660 nm, both from MODIS-Terra and MODIS-Aqua, are overestimated compared to $g_{aer\ (AERONET)}$ at the corresponding wavelengths (stronger overestimation at 870 nm and by Terra). Finally we note an underestimation of g_{aer} at 470 nm from MODIS-Aqua, relative to the data by AERONET at 440 nm, while very small biases (<0.5 %) are found between Terra and AERONET at the same wavelengths.

In Fig. 9 we present a scatterplot comparison between MODIS and AERONET g data pairs. There is bias towards larger g values from both Aqua and Terra compared to AERONET, with Terra overpredicting more than Aqua. The root mean square error to the fit between MODIS and AERONET is very similar between Aqua and Terra. There are concerns on the application of ordinary least squares regression, arising from the assumption that as the assigned independent variable, AERONET values should be free from error. We cannot guarantee the validity of this assumption, so we recognize that the reported R and slope values from Fig. 9 and Table 1, if viewed as metrics of agreement between MODIS g and real g, may be subject to the effect of regression dilution and consequently biased low. This possible bias for R and slope could be neglected only if AERONET errors can also be considered negligible. With the above caveat in mind, the applied least-squares fit line to the scatterplot comparison between matched MODIS-AERONET data pairs (Fig. 9) indicates that MODIS overestimates g_{aer} more in the smaller than larger values, i.e. more for fine than coarse particles.

We present the frequency distributions of asymmetry parameter daily values (Fig. 10) on the days when data from all three databases (MODIS-Terra, MODIS-Aqua and AERONET) were provided. Fig. 10a corresponds to the whole area of interest, while Figs. 10b and c correspond to two broad sub-regions with basic differences in the aerosol source, namely Europe with great anthropogenic sources, and Africa, Middle East and Arabian peninsula, with predominant natural sources and mainly desert dust. There is an apparent skew in the MODIS-Terra and MODIS-Aqua g_{aer} distributions, while the AERONET distributions are more symmetrical. Moreover, the satellite data distributions show larger values and smaller standard deviations compared to AERONET, with the Terra overestimation being more exaggerated. The disagreement

503 is more pronounced in the sub-region of Europe, while in the sub-region of North
504 Africa / Arabian peninsula, the distributions of satellite and surface data agree more
505 thus confirming the finding of Fig. 9 based on the slope of applied linear regression
506 fit. Values over Europe are generally smaller than over North Africa / Arabian
507 peninsula (Fig. 3), which can be attributed to the presence of larger size particles of
508 desert origin in the latter sub-region, in contrast to Europe, where due to industrial
509 activity and frequent biomass burning the presence of smaller size particles is
510 important. Therefore, the smaller g_{aer} values (<0.6) in the frequency distributions of
511 the whole area, are overwhelmingly contributed by the European sub-region,
512 contrasting with larger values (0.7-0.75) being contributed by both sub-regions and
513 even more by N. Africa/Arabian peninsula at larger g_{aer}.

514 Potentially useful results may be derived by the comparison of the temporal trends
515 from satellite and surface data. We show in Fig. 11 the absolute and relative changes
516 of the asymmetry factor, calculated through regression on monthly time series of g_{aer}
517 at 9 AERONET stations with satisfactory temporal coverage of data, selected to have
518 recorded at least 40 monthly values. In the same figure, these variations are compared
519 with corresponding data from MODIS-Terra and MODIS-Aqua, from the 1x1 degree
520 cells containing the locations of the 9 selected stations. We note that we only perform
521 this analysis in a month only if all three datasets give data for the specific month. It
522 should be noted that the g_{aer} changes for these stations do not refer to the same period
523 but they all ensure a complete enough time period enabling thus the derivation of safe
524 conclusions on how MODIS and AERONET changes compare to each other. At five
525 out of the nine stations ("Barcelona", "Dhadnah", "Lecce University", "Rome Tor
526 Vergata" and "Villefranche") the temporal tendencies have the same sign for all three
527 databases, with AERONET showing larger trends. Moreover, the trends are
528 statistically significant at the 95% confidence level for "Barcelona" station.

529 The overall comparison between satellite and surface g_{aer} data performed in the
530 scatterplot of Fig. 9 and Table 1 does not allow one to have an insight to how the
531 comparison behaves spatially, namely how it differs from a region to another. This is
532 addressed in Fig. 12, showing the comparison of satellite and surface data at the
533 wavelength of 870 nm separately between MODIS-Terra - AERONET and MODIS-
534 Aqua – AERONET. For this comparison, we selected AERONET stations for which
535 there is satisfactory overlap between the time series from AERONET and the time
536 series from MODIS, namely the number of common days between AERONET-Terra

and AERONET-Aqua is larger than 100. This intentionally selected less strict criterion that the one used in Fig. 11 is satisfied by 36 stations for AERONET-Terra and by 34 for AERONET-Aqua. For each AERONET station we compute the Pearson correlation coefficient between the station data and the corresponding MODIS-Terra or Aqua data at 870 nm, for the 1°x1° cell containing the station. Moreover, there is the information if the trends between AERONET and either MODIS-Terra or Aqua have the same sign.

In the case of the $g_{aer\ (AERONET)} - g_{aer\ (Terra)}$ comparison, at 5 stations the correlation coefficient R is larger than 0.5, while at 21 stations $0.3<R<0.5$. The largest R found is 0.64 at station "Bahrain". With respect to the agreement on the sign of the trends, at 24 out of 36 stations (67%) there is a trend sign match and at 12 stations (33%) a mismatch. A similar picture emerges for the comparison $g_{aer\ (AERONET)} - g_{aer\ (Aqua)}$. In this case, there are again 5 stations with $R>0.5$ (maximum value $R=0.61$ again at "Bahrain"), while at 19 stations $0.30<R<0.50$. Also, we see that at 22 stations there is a trend sign match and at 12 there is a mismatch (respective percentages equal to 65% and 35%).

5 Summary and Conclusions

Using satellite data from the latest available collection (051) of MODIS-Terra and Aqua data, we examine the spatiotemporal variations of the aerosol asymmetry parameter over North Africa, the Arabian peninsula and Europe. Generally, the largest values of the asymmetry parameter, indicating the strongest forward scattering of radiation by atmospheric aerosols, are found over areas with aerosol load being dominated by large size particles of desert dust (tropical Atlantic, Arabian and Red Seas),. On the contrary, smaller g_{aer} values are seen where a significant fraction of aerosol load comes from small size particles of anthropogenic origin, e.g. over the Black Sea. The results are consistent with the theory and thus prove a good performance of the MODIS retrieval of aerosol asymmetry parameter. Depending on the area of interest, the seasonal cycle of the asymmetry parameter varies markedly. More specifically, in areas with abundance of desert dust particles, the range of intra-annual variation is small, with the largest values during summer, while in other areas the seasonality is reversed, with the largest values during the cold season and the smallest during the warm season. The asymmetry parameter decreases with wavelength, especially when one examines its spatially minimum values, while this

571 decrease is weaker for the larger g_{aer} values, corresponding to the presence of coarser
572 particles.
573 The seasonal fluctuation is more pronounced with increasing wavelength in the
574 examined regions, which is attributed to the different spectral behaviour of the
575 asymmetry parameter for small and large particles. With respect to the inter-annual
576 variability of the asymmetry parameter, we did not discern very important either
577 increasing or decreasing tendencies, with absolute changes smaller than 0.04 in any
578 case. On the other hand, we found opposing tendencies for the two satellite datasets.
579 MODIS-Terra observes mostly increasing tendencies, while Aqua gives extensive
580 regions with decreasing tendencies. Generally, the largest intra-annual and inter-
581 annual variations are seen over the Black Sea, while the smallest over the tropical
582 Atlantic. However, some strong trends (especially from Terra) may be due to
583 calibration drift errors, which may be addressed in collection 006. Along these lines
584 we performed some preliminary comparisons between 051 and 006 Angstrom
585 Exponent trends from Aqua, knowing that AE and g are very closely anti-correlated.
586 These preliminary results, show that 051 Aqua AE trends resemble very closely the
587 006 trends, supporting that the g trends from collection 051 (at least for Aqua)
588 reported in this study are credible.
589 We compare satellite data with surface data from the AERONET, in order to validate
590 the reliability of the former. The quantitative comparison is very useful, since satellite
591 data provide broad geographical coverage and are very important in any study related
592 to aerosols and their climate impact. The disagreement with surface stations can give
593 insights in the resulting errors. Through the examination of frequency distributions of
594 daily g_{aer}, a shift of satellite data towards larger values relative to surface data
595 becomes apparent. This finding is more pronounced for g_{aer} over Europe, while the
596 North African, Arabian peninsula values are more in agreement. Moreover, the
597 smallest g_{aer} values originate from particles from Europe, because of the generation of
598 smaller size particles by industrial activities and biomass burning.
599 In this work we present scatter plots of daily g_{aer} values between MODIS-Terra,
600 MODIS-Aqua, and AERONET, which show moderate agreement between satellite
601 data at 470 nm and surface data at 440 nm, with small correlation coefficients
602 ($R<0.3$). Slightly better agreement was noted at larger wavelengths, but still without
603 reaching very satisfactory levels ($R<0.47$). Nevertheless, during spring and summer,
604 satellite and surface measurements tend to agree more. Finally, for the comparisons at
605 660/675 and 870 nm, we report an overestimation of g_{aer} by MODIS compared to

606 AERONET, as expected because of the less steep decrease of g_{aer} with wavelength of
607 MODIS.

608 We extract pairs of daily Terra-AERONET and Aqua-AERONET values at stations
609 with at least 100 common days. At 21 of 36 stations (Terra-AERONET comparison)
610 and at 19 of 34 stations (Aqua-AERONET comparison) we derive $0.3<R<0.5$, while
611 at 5 stations in both cases, the correlation coefficients are larger than 0.5. Finally, as
612 far as the signs of temporal trends are concerned, we determine agreement in 67%
613 (Terra-AERONET comparison) and in 65% of stations (Aqua-AERONET
614 comparison).

615 The results of the present analysis are useful since they assess for the first time the
616 performance of satellite based products of aerosol asymmetry parameter over broad
617 regions of special climatic interest. Our results can offer an interesting way to assess
618 the uncertainty induced by the use of such satellite g_{aer} data in climate and radiative
619 transfer models that compute aerosol radiative and climate effects. The obtained
620 results are relatively satisfactory given the difficulties encountered by satellite
621 retrieval algorithms due to the different assumptions they made. The identified
622 weaknesses may provide an opportunity to improve such satellite retrievals of aerosol
623 asymmetry parameter in forthcoming data products like those of MODIS C006.

624

625 ## 7 Acknowledgments

626 This research has been co-financed by the European Union (European Social Fund –
627 ESF) and Greek national funds through the operational programme "Education and
628 Lifelong Learning" of the National Strategic Reference Framework (NSRF) –
629 Research Funding Program: THALES. Investing in knowledge society through the
630 European Social Fund. The Collection 005 MODIS-Terra data were obtained from
631 NASA's Level 1 and Atmosphere Archive and Distribution System (LAADS) website
632 (ftp://ladsweb.nascom.nasa.gov/). We would like to thank the principal investigators
633 maintaining the AERONET sites used in the present work.

634

References

Barnaba F. and G. P. Gobbi: Aerosol seasonal variability over the Mediterranean region and relative impact of maritime, continental and Saharan dust particles over the basin from MODIS data in the year 2001, Atmospheric Chemistry and Physics, 4, 4285 - 4337, SRef-ID: 1680-7375/acpd/2004-4-4285SRef-ID: 1680-7375/acpd/2004-4-4285, 2004.

Chubarova, N. Y.: Seasonal distribution of aerosol properties over Europe and their impact on UV irradiance, Atmos. Meas. Tech., 2, 593–608, doi:10.5194/amt-2-593-2009, 2009.

Di Iorio, T., A. di Sarra, W. Junkermann, M. Cacciani, G. Fiocco, and D. Fua, Tropospheric aerosols in the Mediterranean: 1. Microphysical and optical properties, J. Geophys. Res., 108(D10), 4316, doi:10.1029/2002JD002815, 2003

Dubovik, Oleg, Brent Holben, Thomas F. Eck, Alexander Smirnov, Yoram J. Kaufman, Michael D. King, Didier Tanré, Ilya Slutsker, 2002: Variability of Absorption and Optical Properties of Key Aerosol Types Observed in Worldwide Locations. *J. Atmos. Sci.*, **59**, 590–608.

Dubovik, O. and M. D. King, 2000: A flexible inversion algorithm for retrieval of aerosol optical properties from Sun and sky radiance measurements," J. Geophys. Res., 105, 20 673-20 696.

Fotiadi, A., E. Drakakis, N. Hatzianastassiou, C. Matsoukas, K. G. Pavlakis, D. Hatzidimitriou, E. Gerasopoulos, N. Mihalopoulos, and I. Vardavas (2006), Aerosol physical and optical properties in the eastern Mediterranean Basin, Crete, from Aerosol Robotic Network data, Atmos. Chem. Phys., 6, 5399– 5413.

Gerasopoulos, E., Kouvarakis, G., Babasakalis, P., Vrekoussis, M., Putaud, J. P., and Mihalopoulos, N.: Origin and variability of particulate matter (PM10) mass concentrations over the Eastern Mediterranean, Atmos. Environ., 40, 4679–4690, 2006.

Gkikas, A., Hatzianastassiou, N., and Mihalopoulos, N.: Study and characterization of aerosol episodes in the Mediterranean basin for the 7-year period 2000–2007 based on MODIS data, European Aerosol Conference, Greece, Thessaloniki, 24–29 August 2008.

Gkikas, A., Hatzianastassiou, N., and Mihalopoulos, N.: Aerosol events in the broader Mediterranean basin based on 7-year (2000–2007) MODIS C005 data, Ann. Geophys., 27, 3509–3522, doi:10.5194/angeo-27-3509-2009, 2009.

Gkikas, A., Houssos, E., Hatzianastassiou, N., Papadimas, C. and Bartzokas, A. (2011), Synoptic conditions favouring the occurrence of aerosol episodes over the broader Mediterranean basin. Q.J.R. Meteorol. Soc.. doi: 10.1002/qj.978

Goloub, P., and O. Arino, 2000: Verification of the consistency of POLDER aerosol index over land with ATSR-2 fire product. Geophys. Res. Lett., 27, 899–902.

Graßl, H.: Possible changes of planetary albedo due to aerosol particles, in Man's Impact on Climate, edited by: W. Bach, J. Pankrath, and W. Kellogg, Elsevier, New York, 1979.

672 Hansen, J., Sato, M., and Ruedy, R.: Radiative forcing and climate response, J. Geophys.
673 Res., 102, 6831–6864, 1997.
674 Hatzianastassiou, N., B. Katsoulis, I. Vardavas: Sensitivity analysis of aerosol direct radiative
675 forcing in ultraviolet - visible wavelengths and consequences for the heat budget, Tellus,
676 56b, 368 - 381, 2004.
677 Hatzianastassiou, N., A. Gkikas, N. Mihalopoulos, O. Torres, and B. D. Katsoulis: Natural
678 versus anthropogenic aerosols in the eastern Mediterranean basin derived from multiyear
679 TOMS and MODIS satellite data, J. Geophys. Res., 114, D24202,
680 doi:10.1029/2009JD011982, 2009.
681 Hatzianastassiou, N., Matsoukas, C., Drakakis, E., Stackhouse Jr., P. W., Koepke, P.,
682 Fotiadi, A., Pavlakis, K. G., and Vardavas, I.: The direct effect of aerosols on solar
683 radiation based on satellite observations, reanalysis datasets, and spectral aerosol optical
684 properties from Global Aerosol Data Set (GADS), Atmos. Chem. Phys., 7, 2585-2599,
685 doi:10.5194/acp-7-2585-2007, 2007.
686 Haywood, J.M., and O. Boucher, 2000: Estimates of the direct and indirect radiative forcing
687 due to tropospheric aerosols: A review.Rev. Geophys., 38, 513–543.
688 Heishman, J. (1999), Commanding Officer, Forecaster's Handbook, U.S. Navy Cent.
689 Meteorol. and Oceanogr. Cent., Manama, Bahrain.
690 Holben B.N., T.F. Eck, I. Slutsker, D. Tanré, J.P. Buis, A. Setzer, E. Vermote, J.A. Reagan,
691 Y. Kaufman, T. Nakajima, F. Lavenu, I. Jankowiak, and A. Smirnov, 1998: AERONET -
692 A federated instrument network and data archive for aerosol characterization, Rem. Sens.
693 Environ., 66, 1-16.
694 Ichoku C., D. Allen Chu,Shana Mattoo,Yoram J. Kaufman, Lorraine A. Remer, Didier
695 Tanre´, Ilya Slutsker, and Brent N. Holben: A spatio-temporal approach for global
696 validation and analysis of MODIS aerosol products. GEOPHYSICAL RESEARCH
697 LETTERS, VOL. 29, NO. 12, 10.1029/2001GL013206, 2002.
698 IPCC, 2007: Climate Change 2007: The Physical Science Basis. Contribution of Working
699 Group I to the Fourth Assessment Report of the Intergovernmental Panel on Climate
700 Change [Solomon, S., D. Qin, M. Manning, Z. Chen, M. Marquis, K.B. Averyt, M.Tignor
701 and H.L. Miller (eds.)]. Cambridge University Press, Cambridge, United Kingdom and
702 New York, NY, USA.
703 IPCC, 2013: Climate Change 2013: The Physical Science Basis. Contribution of Working
704 Group I to the Fifth Assessment Report of the Intergovernmental Panel on Climate Change
705 [Stocker, T.F., D. Qin, G.-K. Plattner, M. Tignor, S.K. Allen, J. Boschung, A. Nauels, Y.
706 Xia, V. Bex and P.M. Midgley (eds.)]. Cambridge University Press, Cambridge, United
707 Kingdom and New York, NY, USA, 1535 pp.
708 Jianrong Bi, Jianping Huang, Qiang Fu, Xin Wanga, Jinsen Shi , Wu Zhang , Zhongwei
709 Huang, Beidou Zhang: Toward characterization of the aerosol optical properties over

710 Loess Plateau of Northwestern China. Journal of Quantitative Spectroscopy & Radiative
711 Transfer 112 (2011) 346–360
712 Kalivitis, N., Gerasopoulos, E., Vrekoussis, M., Kouvarakis, G., Kubilay, N.,
713 Hatzianastassiou, N., Vardavas, I., and Mihalopoulos, N.: Dust transport over the eastern
714 Mediterranean derived from TOMS, AERONET and surface measurements, J. Geophys.
715 Res., 112, D03202, doi:10.1029/2006JD007510, 2007.
716 Kaufman, Y. J., D. Tanré, L. A. Remer, E. F. Vermote, A. Chu, and B. N. Holben:
717 Operational remote sensing of tropospheric aerosol over land from EOS moderate
718 resolution imaging spectroradiometer, J. Geophys. Res., 102, 17,051– 17,067, 1997.
719 Kinne, S., D. O'Donnel, P. Stier, S. Kloster, K. Zhang, H. Schmidt, S. Rast, M. Giorgetta, T.
720 F. Eck, and B. Stevens (2013), MAC-v1: A new global aerosol climatology for climate
721 studies, J. Adv. Model. Earth Syst., 5, 704–740, doi:10.1002/jame.20035.
722 Koepke, P., M. Hess, I.Schult, and E. P. Shettle: Global aerosol data set, Rep. No. 243, Max-
723 Planck Institut fuer Meteorologie, Hamburg, Germany, 44 pp., 1997.
724 Lelieveld, J., et al. (2002), Global air pollution crossroads over the Mediterranean, Science,
725 298, 794– 799, doi:10.1126/science.1075457.
726 Lohmann U., Feichter, J. [2005] Global indirect aerosol effects: A review . Atmos. Chem.
727 Phys., 5, 715-737
728 Lyamani, H., F. J. Olmo, A. Alca´ntara, and L. Alados-Arboledas (2006), Atmospheric
729 aerosols during the 2003 heat wave in southeastern Spain. I: Spectral optical depth, Atmos.
730 Environ., 40, 6453 – 6464, doi:10.1016/ j.atmosenv.2006.04.048.
731 Papadimas, C. D., N. Hatzianastassiou, N. Mihalopoulos, X. Querol, and I.
732 Vardavas (2008), Spatial and temporal variability in aerosol properties over the
733 Mediterranean basin based on 6-year (2000–2006) MODIS data, J. Geophys. Res., 113,
734 D11205, doi:10.1029/2007JD009189.
735 Pace, G., A. di Sarra, Meloni, D., Piacentino, S., and Chamard, P.: Aerosol optical
736 properties at Lampedusa (Central Mediterranean). 1. Influence of transport and
737 identification of different aerosol types, Atmos. Chem. Phys., 6, 697–713, 2006,
738 www.atmos-chem-phys.net/6/697/2006/.
739 Pandithurai, R. T. Pinker, P. C. S. Devara, T. Takamura, K. K. Dani, Seasonal asymmetry in
740 diurnal variation of aerosol optical characteristics over Pune, western India, J. Geophys.
741 Res., 112, D8, DOI: 10.1029/2006JD007803, 2007.
742 Prospero, J., P. Ginoux, O. Torres, and S. E. Nicholson (2002), Environmental
743 Characterization of Global sources of atmospheric soil dust derived from the NIMBUS-7
744 TOMS absorbing aerosol product, Rev. Geophys., 40(1), 1002,
745 doi:10.1029/20000GR000095.
746 Remer L.A., Kaufman Y.J., Tanre D. and co-authors: The MODIS aerosol algorithm,
747 products, and validation, J. Atmos. Sci., 62: 947-973, 2005.

748 Remer LA, Kleidman RG, Levy RC, Kaufman YJ, Tanr'e D, Mattoo S, Martins JV, Ichoku
749 C, Koren I, Yu H, Holben BN. 2008. Global aerosol climatology from the MODIS satellite
750 sensors. Journal of Geophysical Research 113: D14S07, DOI: 10.1029/2007JD009661.
751 Satheesh, S. K., V. Ramanathan, X. Li-Jones, J. M. Lobert, I. A. Podgorny, J. M. Prospero, B.
752 N. Holben, and N. G. Loeb, A model for the natural and anthropogenic aerosols over the
753 tropical Indian Ocean derived from Indian Ocean Experiment data, J. Geophys. Res., 104,
754 27,421–27,440, 1999.
755 Savoie, D. L., J. M. Prospero, and R. T. Nees, Nitrate, nonsea-salt sulfate, and mineral
756 aerosolover the northwestern Indian Ocean, J. Geophys. Res., 92, 933–942, 1987.
757 Sciare, J., H. Bardouki, C. Moulin, and N. Mihalopoulos (2003), Aerosol sources and their
758 contribution to the chemical composition of aerosols in the Eastern Mediterranean Sea
759 during summertime, Atmos. Chem. Phys., 3, 291–302, SRef-ID:1680 – 7324/acp/2003–3-
760 291.
761 Smirnov, A., B. N. Holben, Y. J. Kaufman, O. Dubovik, T. F. Eck, I. Slutsker, C. Pietras, and
762 R. N. Halthore, 2002b: Optical properties of atmospheric aerosol in maritime
763 environments. *J. Atmos. Sci.,* **59,** 501–523.
764 Snirnov, and Coauthors, 2002a: Atmospheric aerosol optical properties in the Persian Gulf. J.
765 Atmos. Sci., 59, 620–634.
766 Smirnov, A., B. N. Holben, T. F. Eck, I. Slutsker, B. Chatenet, and R. T. Pinker,
767 2002c: Diurnal variability of aerosol optical depth observed at AERONET
768 (Aerosol Robotic Network) sites, *Geophys. Res. Lett.,* **29,** 23, 2115,
769 doi:10.1029/2002GL016305.
770 Tanré, D., Y. J. Kaufman, M. Herman, and S. Mattoo: Remote sensing of aerosol properties
771 over oceans using the MODIS/EOS spectral radiances, J. Geophys. Res., 102, 16,971–
772 16,988, 1997.
773 Tindale, N. W., and P. P. Pease, Aerosols over the Arabian Sea: Atmospheric transport
774 pathways and concentrations of dust and sea salt, Deep Sea Res., 46, 1577–1595, 1999.
775 Yu, H., Dickinson, R. E., Chin, M., Kaufman, Y. J., Holben, B. N. Geogdzhayev, I. V., and
776 Mishchenko, M. I.: Annual cycle of global distributions of aerosol optical depth from
777 integration of MODIS retrievals and GOCART model simulations, J. Geophys. Res., 108,
778 4128, doi:10.1029/2002JD002717, 2003.
779 Zdun, A., A. Rozwadowska and S. Kratzer, 2011. Seasonal variability in the optical
780 properties of Baltic aerosols, Oceanologia, 53(1), 7-34.
781
782

783 **Table 1.** Correlation coefficients (R), mean bias, root mean squared error (RMSE)
784 and the slope and intercept values of applied linear regression fits between MODIS
785 and AERONET g_{aer} data. The statistical parameters are given separately for the pairs
786 of wavelengths: (i) 470 nm (MODIS) and 440 nm (AERONET), (ii) 660 nm
787 (MODIS) and 675nm (AERONET) and (iii) 870 nm (MODIS and AERONET). The
788 statistical parameters are also given separately for winter, spring, summer and
789 autumn.[a]

790

791 *MODIS-Terra*
792

		R	Bias*	RMSE	Slope	Intercept
year	470-440	0.25	$2x10^{-4}$	0.045	0.36	0.45
	660-675	0.41	-0.028	0.060	0.55	0.32
	870	0.47	-0.035	0.070	0.60	0.29
Winter	470-440	0.20	$4.5x10^{-4}$	0.046	0.26	0.53
	660-675	0.35	-0.033	0.056	0.41	0.42
	870	0.41	-0.053	0.057	0.40	0.43
Spring	470-440	0.27	$-5x10^{-4}$	0.046	0.40	0.43
	660-675	0.44	-0.023	0.060	0.63	0.27
	870	0.50	-0.026	0.071	0.67	0.24
Summe	470-440	0.33	-0.002	0.044	0.51	0.35
	660-675	0.48	-0.031	0.061	0.71	0.22
	870	0.54	-0.030	0.077	0.79	0.16
Autumn	470-440	0.21	0.003	0.044	0.30	0.50
	660-675	0.33	-0.027	0.059	0.45	0.38
	870	0.41	-0.035	0.068	0.53	0.34

793
794
795 *MODIS-Aqua*
796

		R	Bias*	RMSE	Slope	Intercept
	470-440	0.27	0.018	0.047	0.41	0.40
	660-675	0.42	-0.005	0.062	0.61	0.26
	870	0.46	-0.015	0.072	0.61	0.26
Win	470-440	0.25	0.024	0.049	0.36	0.43

[a] The reported correlation coefficients and slopes may be biased low, because we did not include in our analysis the unknown AERONET errors.

ter						
	660-675	0.39	-0.001	0.062	0.55	0.30
	870	0.43	-0.021	0.068	0.51	0.33
Spring	470-440	0.29	0.015	0.048	0.45	0.38
	660-675	0.45	-0.003	0.064	0.70	0.20
	870	0.50	-0.007	0.076	0.71	0.19
Summe	470-440	0.35	0.014	0.045	0.55	0.30
	660-675	0.50	-0.012	0.060	0.72	0.19
	870	0.53	-0.018	0.074	0.73	0.19
Autumn	470-440	0.20	0.021	0.047	0.30	0.47
	660-675	0.32	-0.003	0.061	0.46	0.36
	870	0.37	-0.014	0.069	0.48	0.34

797
798 * $g_{aer(AERONET)}$-$g_{aer(MODIS)}$
799

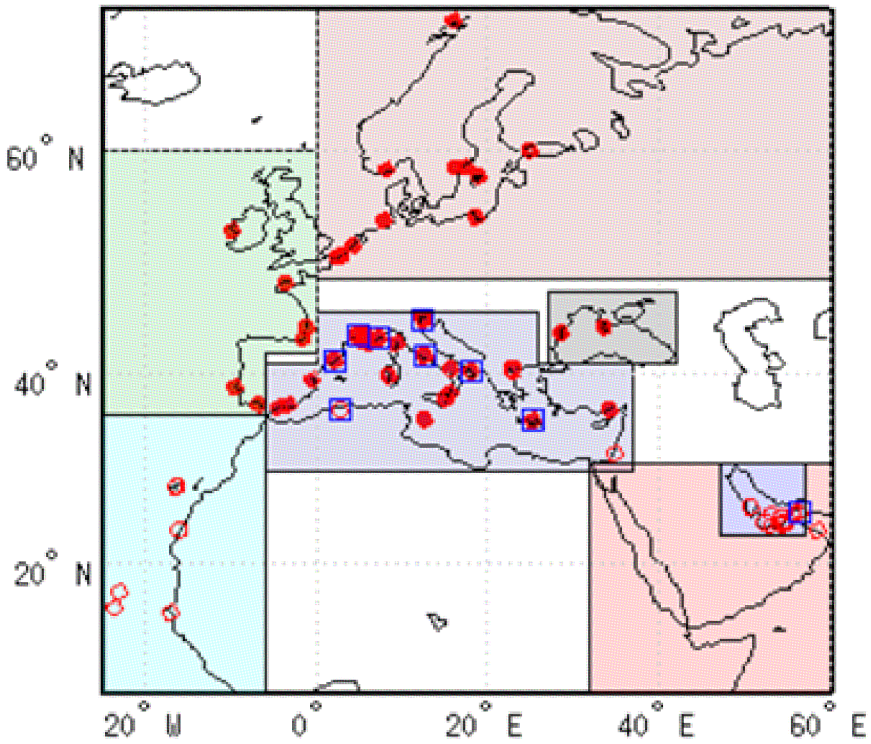

Figure 1. Comparison between HAC and MODIS total aerosol optical depth at 550nm. Global seasonal distribution of relative percentage differences ((HAC-MODIS)/MODIS -%) for: (a) winter (December-January-February), (b) spring (March-April-May), (c) summer (June-July-August) and (d) autumn (September-October-November). White shaded areas correspond to cases for which MODIS AOD values are missing or do not qualify for the averaging threshold.

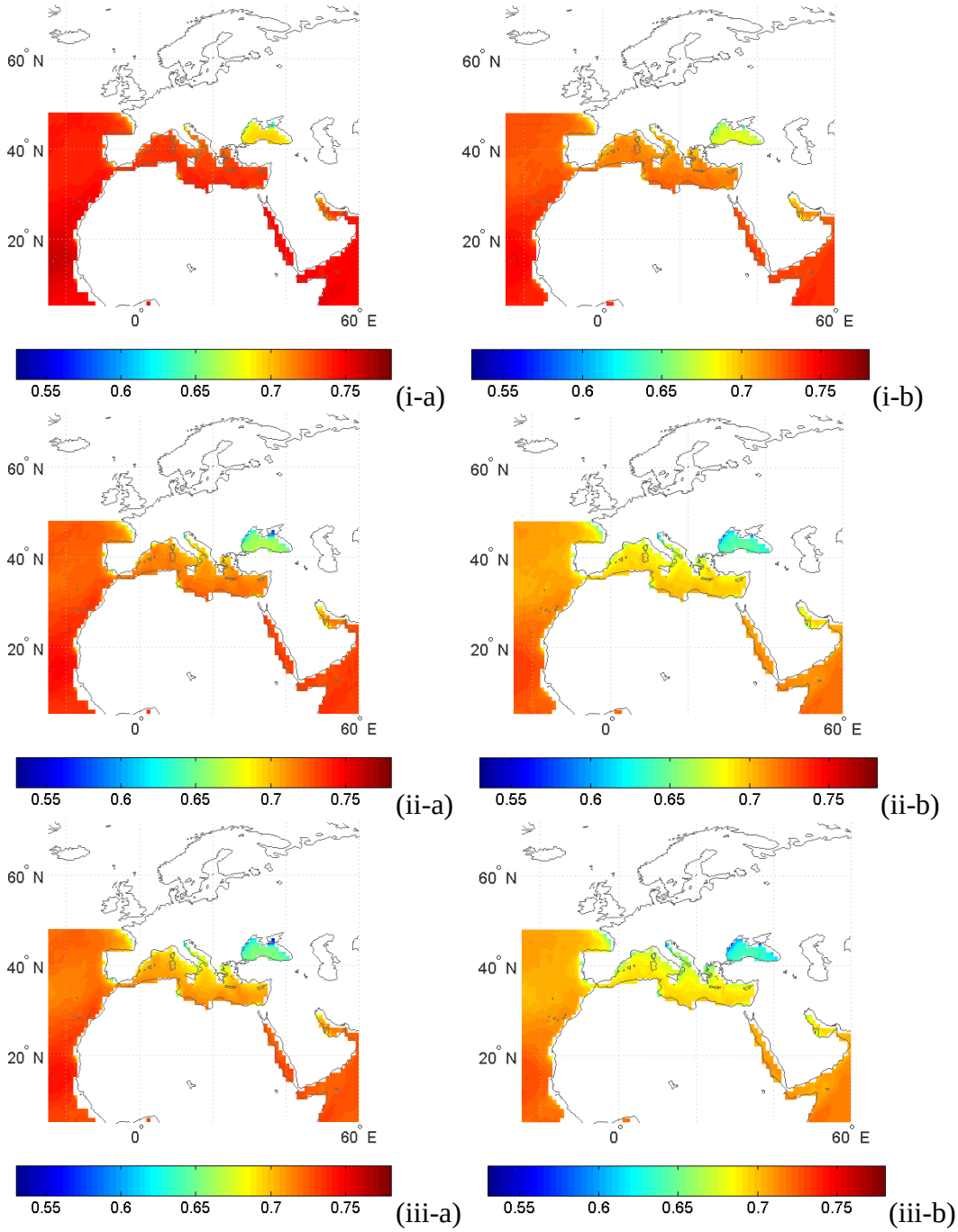

Figure 2. Geographical distribution of MODIS-Terra (-a, left column) and MODIS-Aqua (-b, right column) g_{aer} values averaged over 2002-2010, at the wavelengths of: 470 nm (i-, top row), 660 nm (ii-, middle row) and 870 nm (iii-, bottom row).

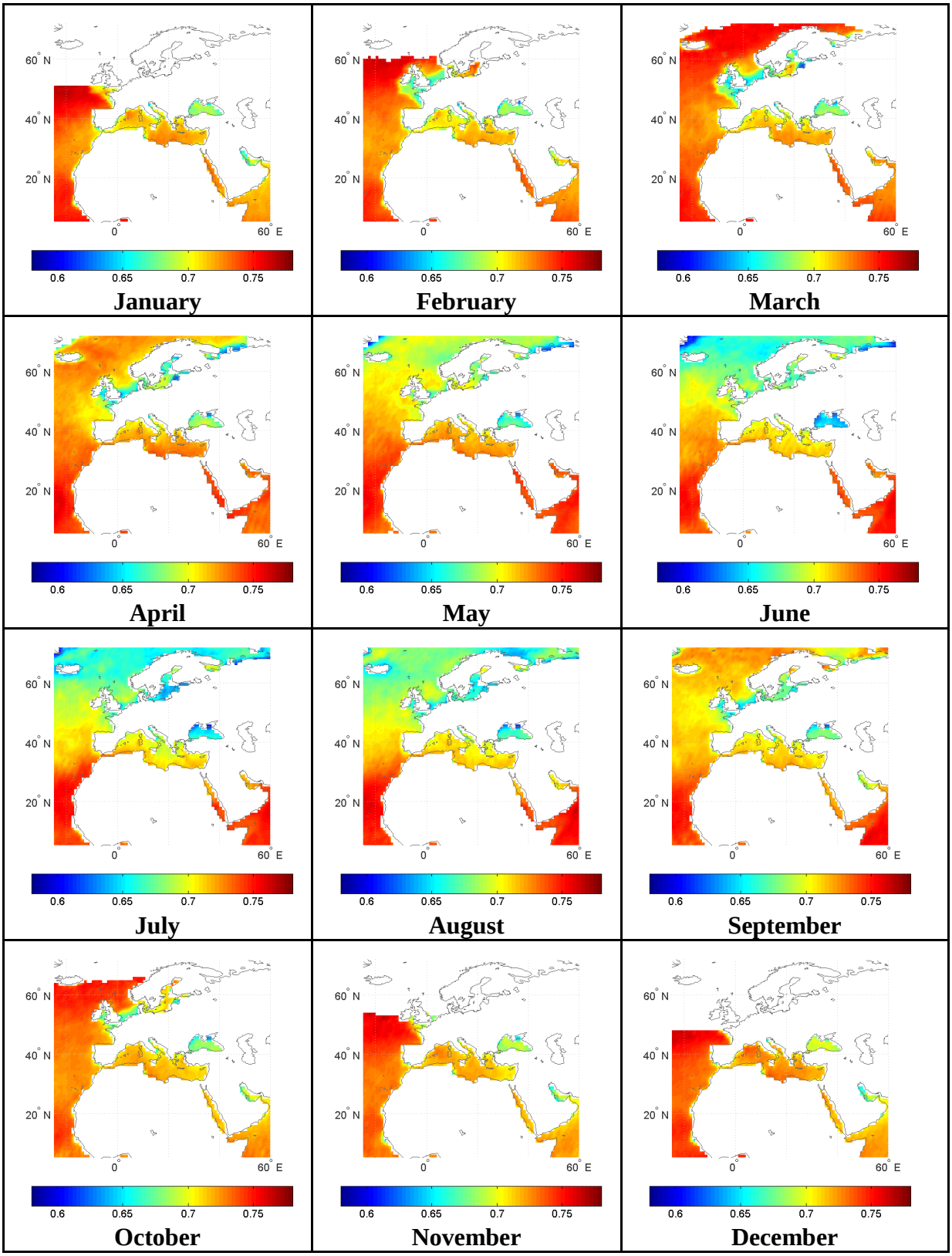

Figure 3. Month by month variation of MODIS-Aqua g_{aer} values at 470 nm averaged over the period 2002-2010.

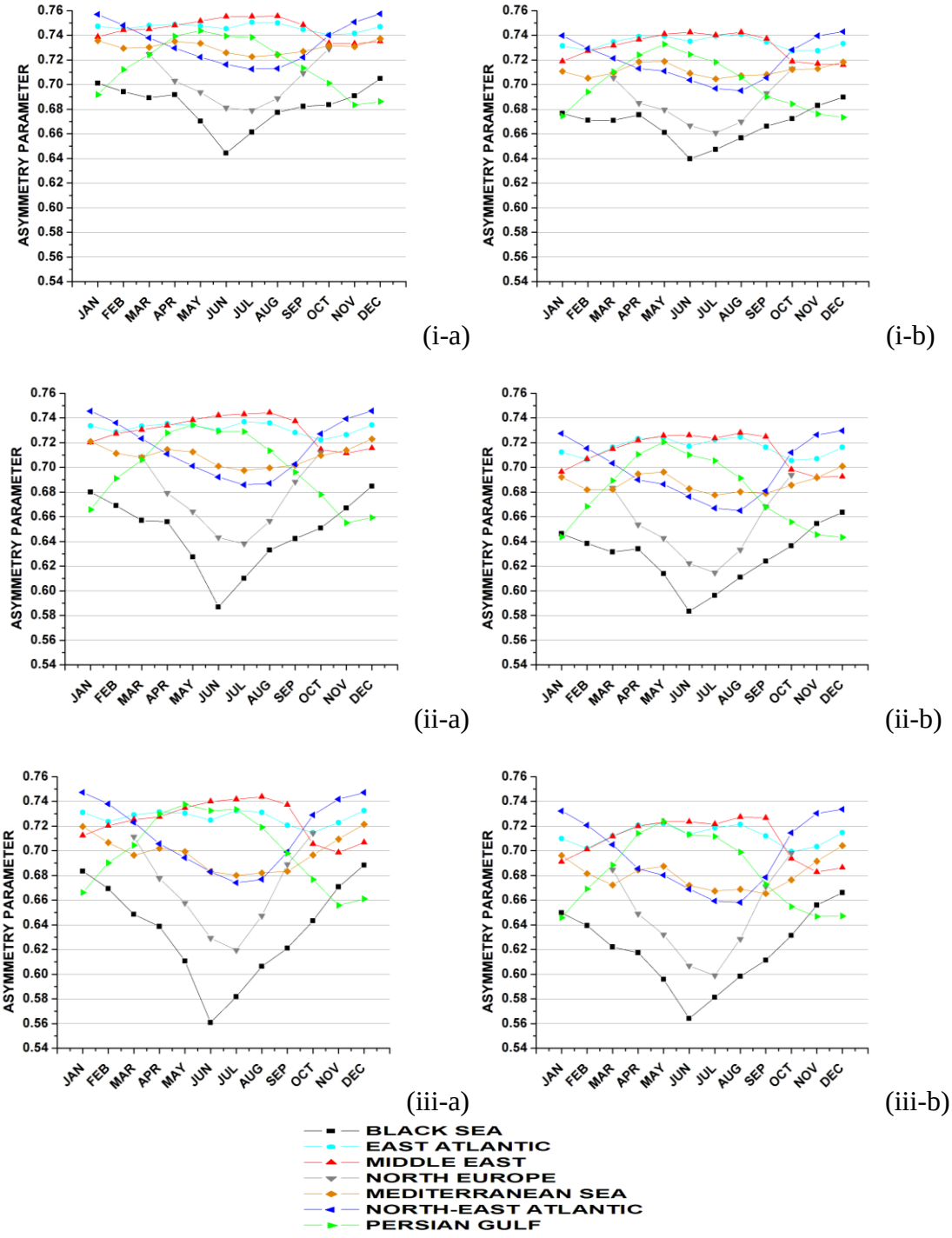

Figure 4. Intra-annual variation of MODIS Terra (-a, left column) and Aqua (-b, right column) g_{aer} values averaged over seven selected sub-regions (Fig. 1). Results are given for g_{aer} values at: 470 nm (i-, top row), 660 nm (ii-, middle row) and 870 nm (iii-, bottom row), averaged over the period 2002-2010, respectively.

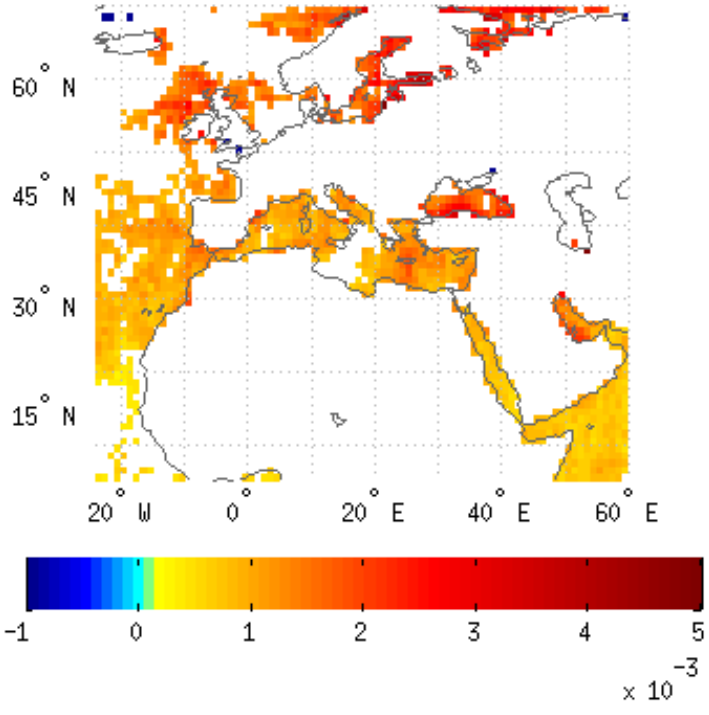

(a)

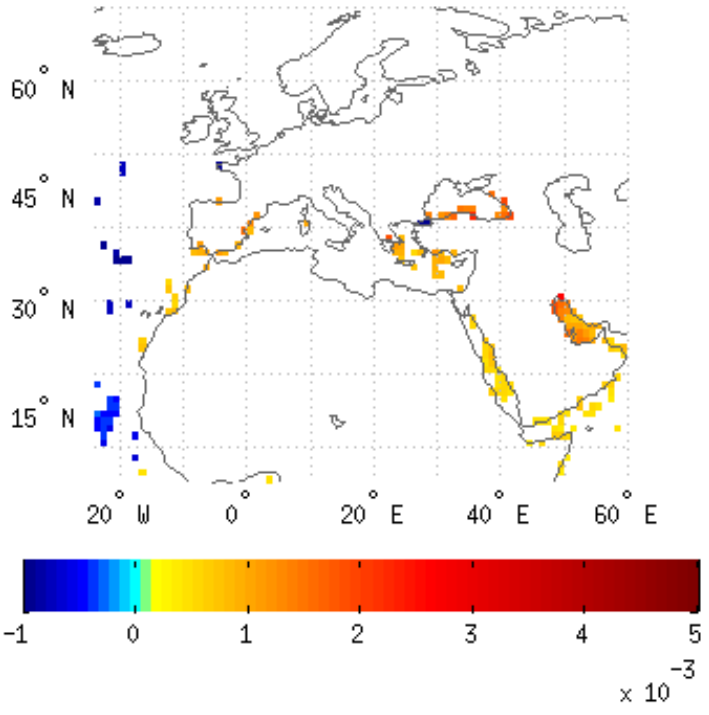

(b)

Figure 5. Slope (in units decade^{-1}) of MODIS g_{aer} deseasonalized anomalies over the period 2002-2010 from MODIS-Terra (-a, top) and MODIS-Aqua (-b, bottom), for the wavelengths of 470 nm.

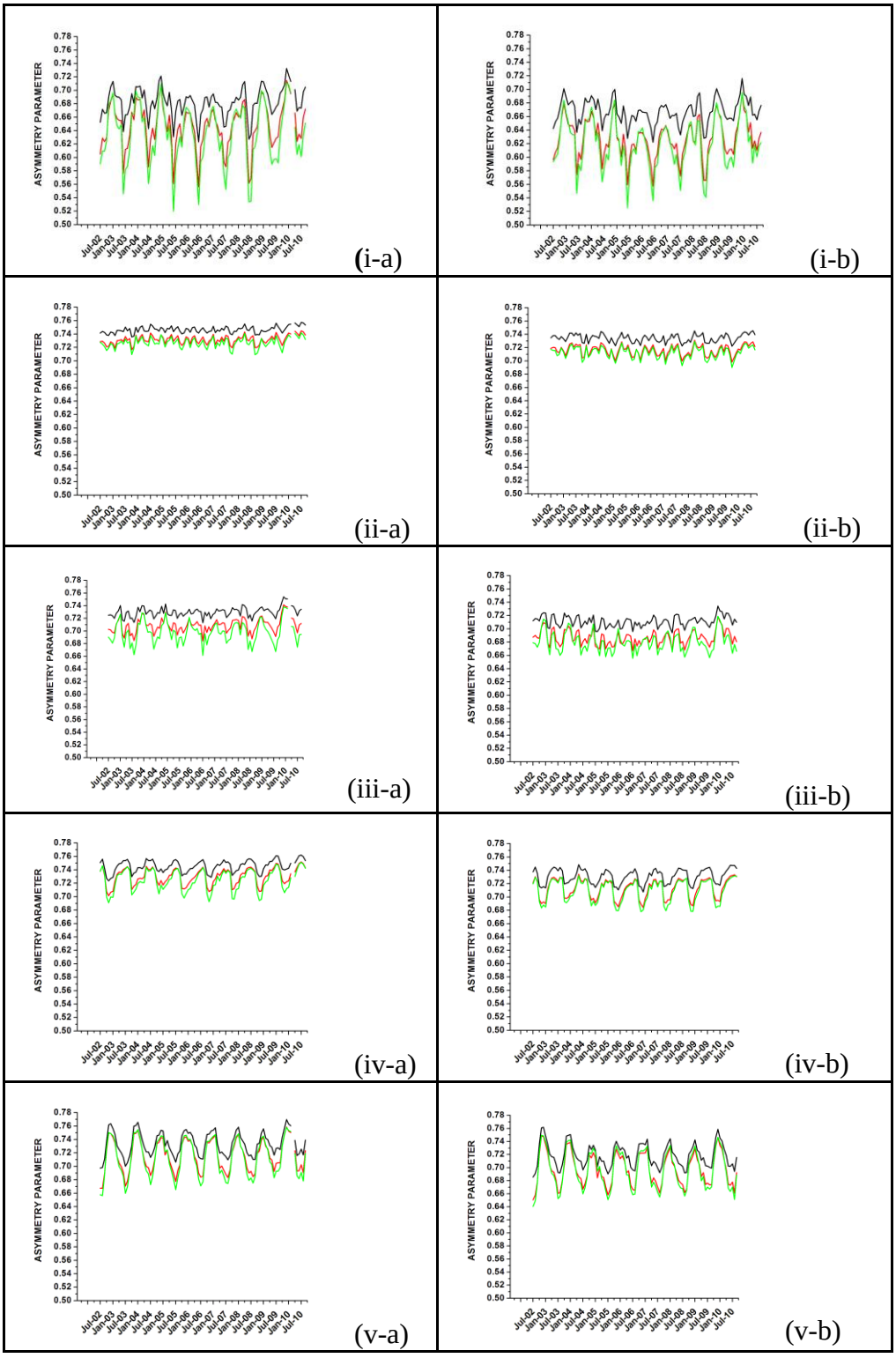

840

841 **Figure 6.** Inter-annual (2002-2010) variation of monthly mean g_{aer} values at 470 nm
842 averaged over the sub-regions of: (i) Black Sea, (ii) Eastern Atlantic Ocean, (iii)
843 Mediterranean Sea, (iv) Middle East, (v) North-eastern Atlantic Ocean, (vi) North
844 Europe and (vii) Persian Gulf. Results are given based on MODIS-Terra (-a, left
845 column) and MODIS-Aqua (-b, right column).

846

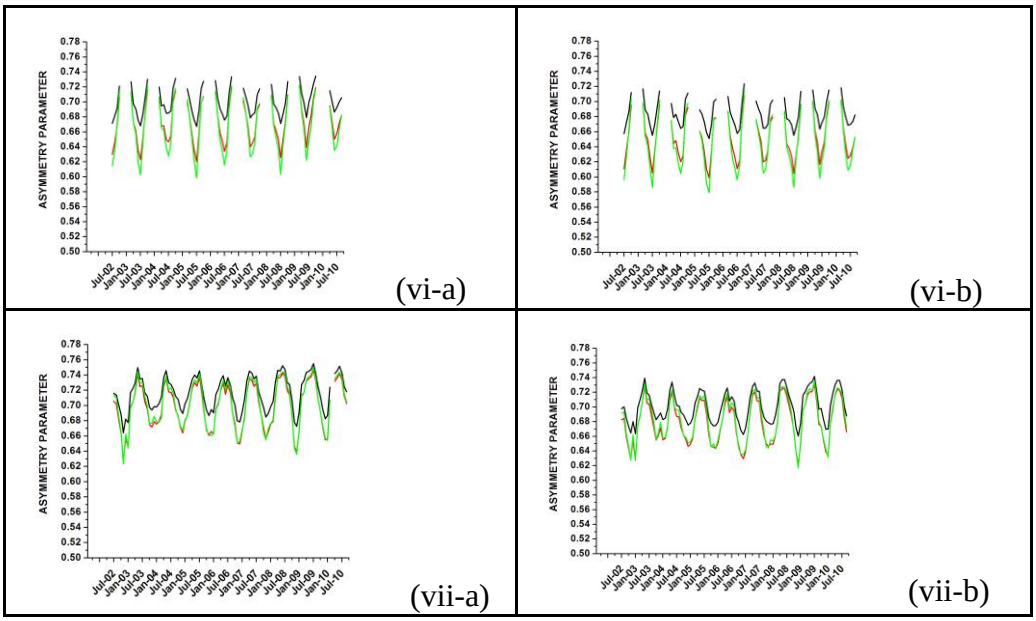

Figure 6 (continued). Inter-annual (2002-2010) variation of monthly mean g_{aer} values at 470 nm averaged over the sub-regions of: (i) Black Sea, (ii) Eastern Atlantic Ocean, (iii) Mediterranean Sea, (iv) Middle East, (v) North-eastern Atlantic Ocean, (vi) North Europe and (vii) Persian Gulf. Results are given based on MODIS-Terra (-a, left column) and MODIS-Aqua (-b, right column).

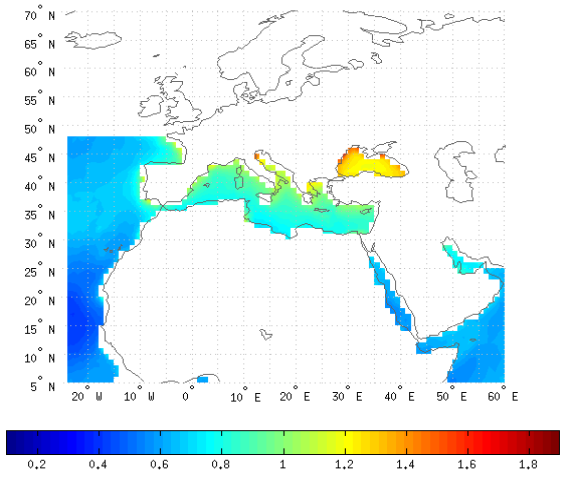

(a)

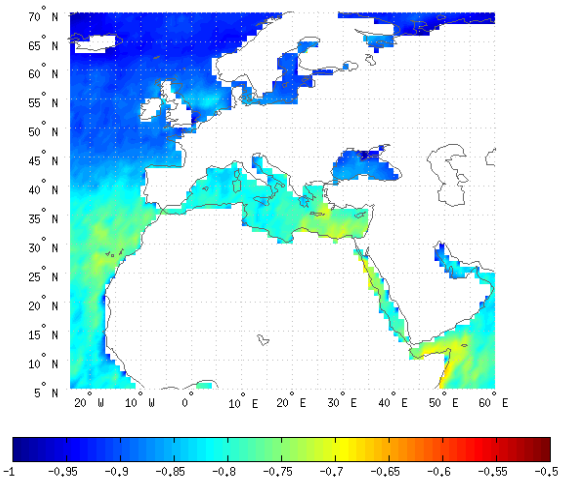

(b)

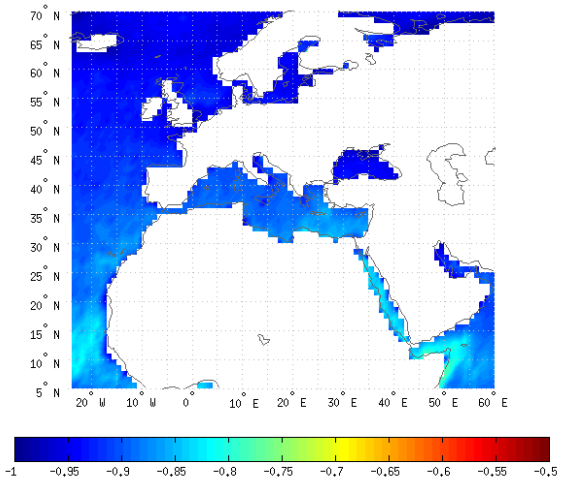

(c)

Figure 7. Geographical distribution of MODIS-Aqua C005 Angström exponent ($AE_{550\text{-}865}$) values averaged over 2002-2010, at the wavelength pair of 550-865 nm. The correlation coefficients between $AE_{550\text{-}865}$ and g_{aer} data at 660 and 870 nm are given in (b) and (c), respectively.

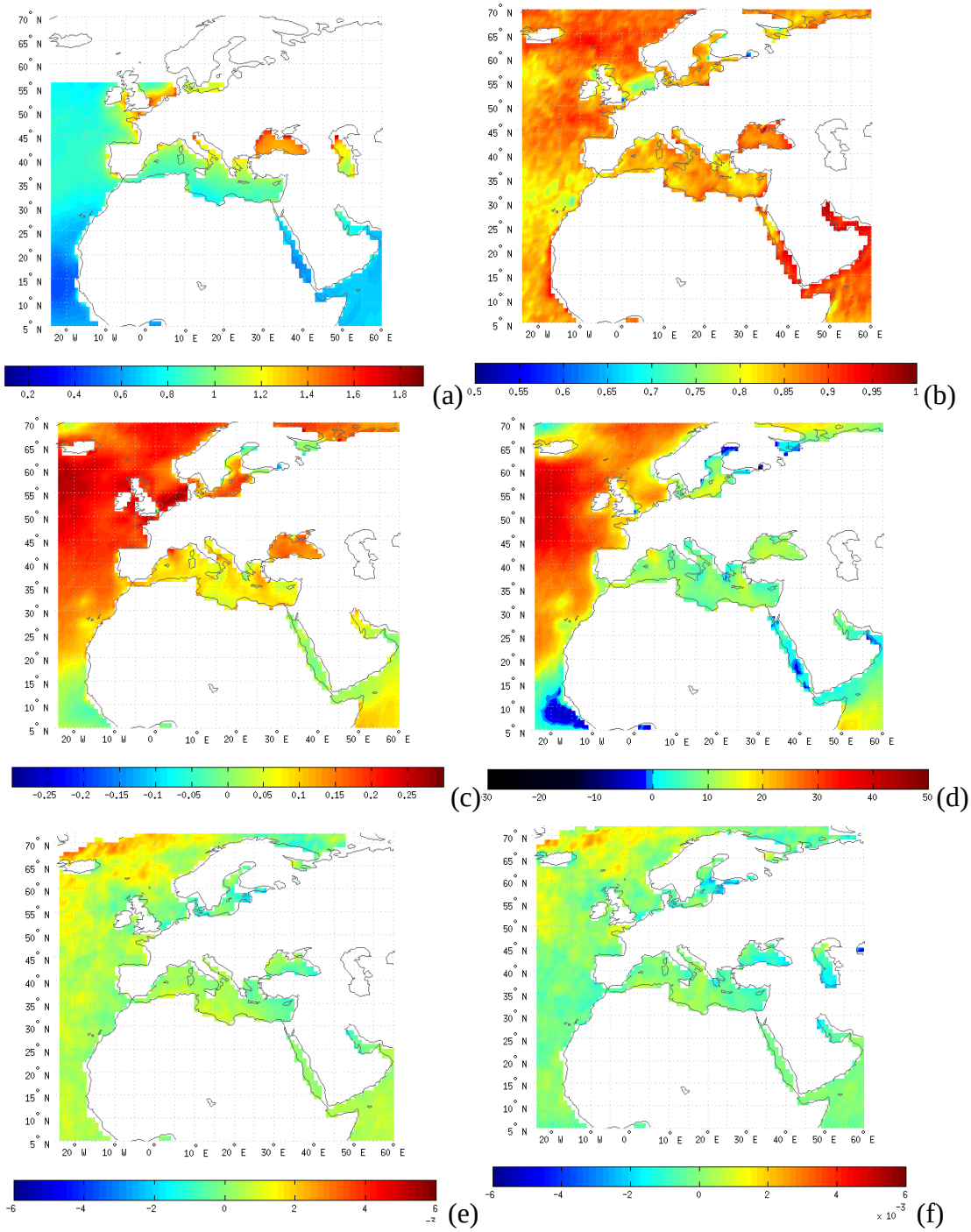

Figure 8. Geographical distribution of MODIS-Aqua C006 Angström exponent ($AE_{550\text{-}865}$) values averaged over 2002-2010, at the wavelength pair of 550-865 nm. In (b), (c) and (d) are given the correlation coefficients, the absolute biases and the relative percent biases, respectively, between the C006 and corresponding C005 $AE_{550\text{-}865}$ data. In (e) and (f) are given the computed deseasonalized trends of MODIS Aqua C005 and C006 $AE_{550\text{-}865}$) slope values for years 2002-2010, respectively.

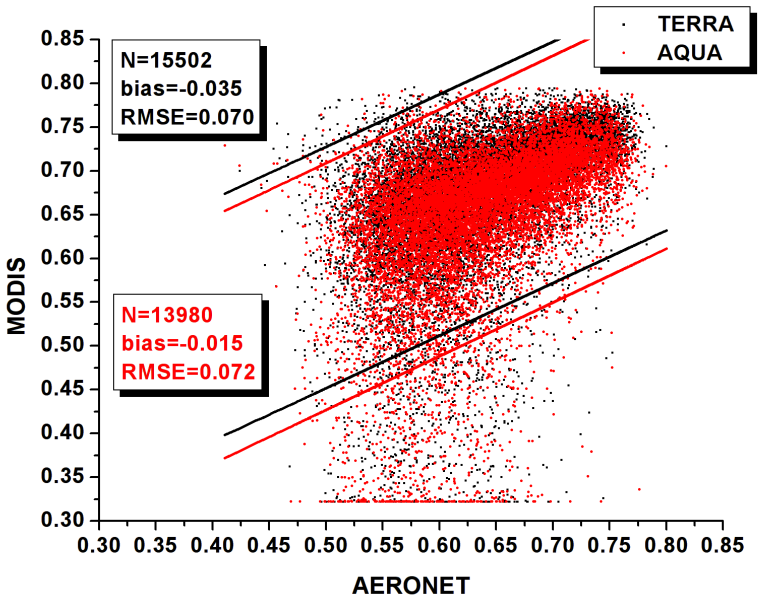

875
876
877 **Figure 9.** Scatterplot comparison between g_{aer} values at 870 nm from MODIS Terra
878 (black color) and Aqua (red color) and corresponding values from AERONET stations
879 (blue squares, Fig. 1). The 95% prediction bands as well as the mean bias and root
880 mean squared error are given.

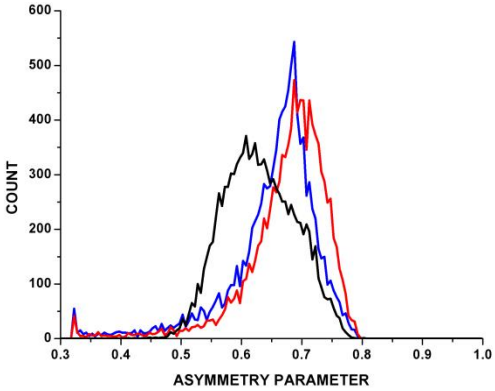

(a)

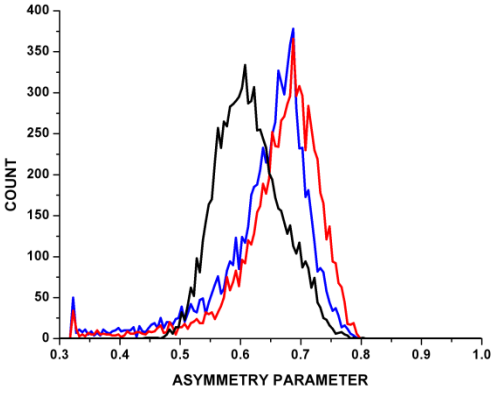

(b)

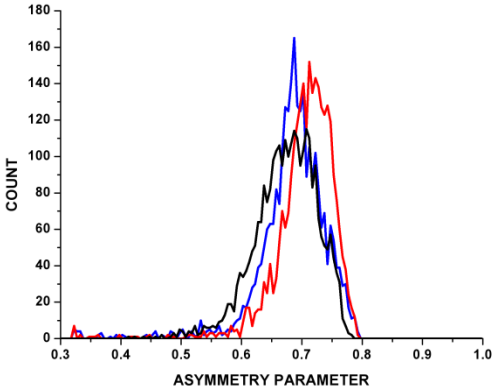

(c)

Figure 10. Frequency distribution histograms for MODIS-Terra (red colored lines) MODIS-Aqua (blue-colored lines) and AERONET (black lines) g_{aer} values at 870 nm. The histograms are given separately for: (a) the entire study region, (b) Europe and (c) Africa, Middle East and Arabian peninsula.

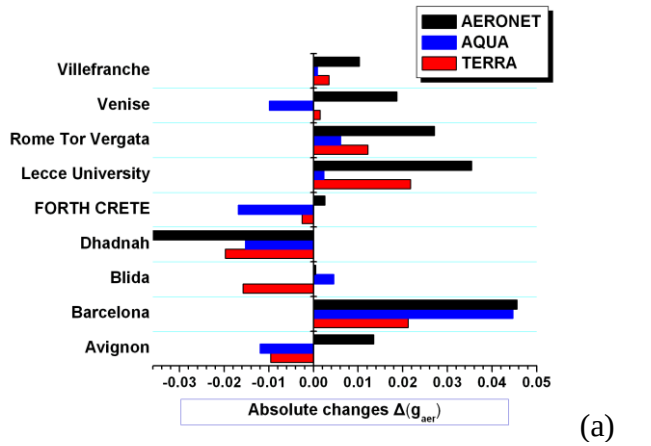

(a)

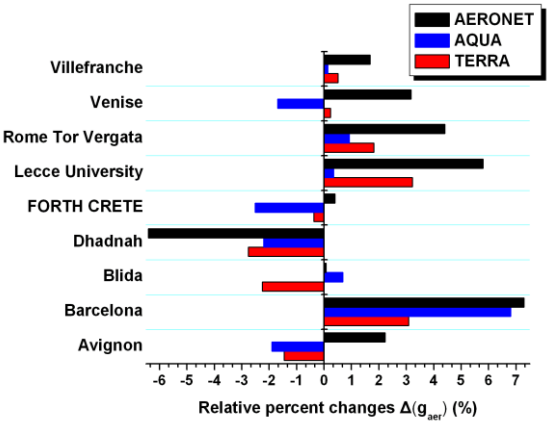

(b)

Figure 11. Frequency distribution histograms for MODIS-Terra (red colored lines) MODIS-Aqua (blue-colored lines) and AERONET (black lines) g_{aer} values at 870 nm. The histograms are given separately for: (a) the entire study region, (b) Europe and (c) Africa, Middle East and Arabian peninsula.

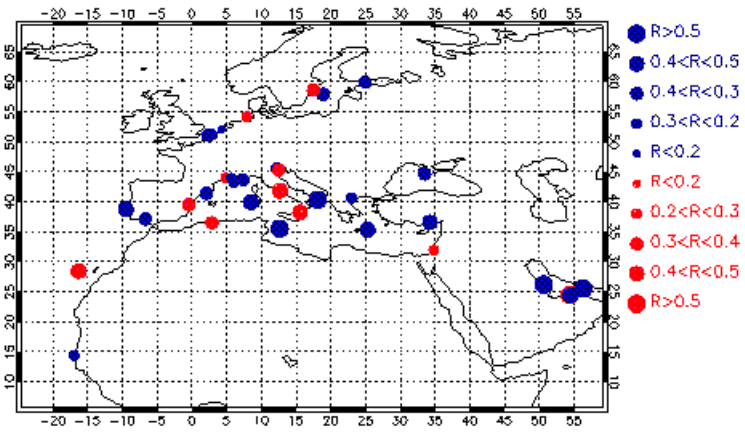

(a)

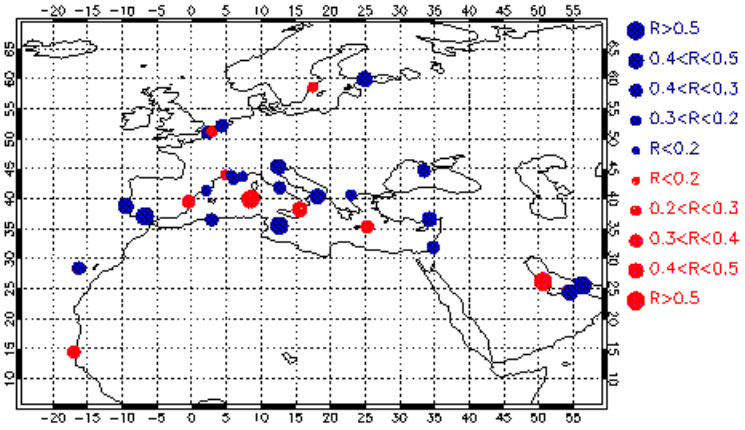

(b)

Figure 12. Map distribution of correlation coefficients between: (i) MODIS-Terra and AERONET g_{aer} values at 870 nm (left column) and (ii) MODIS-Aqua and AERONET g_{aer} values at 870 nm (right column). The size of circles corresponds to the magnitude of correlation coefficients, while blue and red colors are used for stations for which MODIS and AERONET indicate same and opposite tendency of g_{aer}, respectively.